Article

Predicting Lifestyle from Positive Selection Data and Genome Properties in Oomycetes

Daniel Gómez-Pérez (ID) **and Eric Kemen *** (ID)

Center for Plant Molecular Biology (ZMBP), University of Tübingen, 72074 Tübingen, Germany;
daniel.gomez-perez@uni-tuebingen.de
* Correspondence: eric.kemen@uni-tuebingen.de; Tel.: +49-7071-29-78725

Abstract: As evidenced in parasitism, host and niche shifts are a source of genomic and phenotypic diversification. Exemplary is a reduction in the core metabolism as parasites adapt to a particular host, while the accessory genome often maintains a high degree of diversification. However, selective pressures acting on the genome of organisms that have undergone recent lifestyle or host changes have not been fully investigated. Here, we developed a comparative genomics approach to study underlying adaptive trends in oomycetes, a eukaryotic phylum with a wide and diverse range of economically important plant and animal parasitic lifestyles. Our analysis reveals converging evolution on biological processes for oomycetes that have similar lifestyles. Moreover, we find that certain functions, in particular carbohydrate metabolism, transport, and signaling, are important for host and environmental adaptation in oomycetes. Given the high correlation between lifestyle and genome properties in our oomycete dataset, together with the known convergent evolution of fungal and oomycete genomes, we developed a model that predicts plant pathogenic lifestyles with high accuracy based on functional annotations. These insights into how selective pressures correlate with lifestyle may be crucial to better understand host/lifestyle shifts and their impact on the genome.

Keywords: oomycetes; lifestyle; evolution

1. Introduction

The adaptation of organisms as they evolve to occupy different niches or adopt different lifestyles is reflected in their genome. Expansion or contraction of gene families has been cited as a general mechanism for such adaptations [1,2]. Expansions arise mainly from gene duplication and, in some cases, from acquisition via horizontal gene transfer, whereas gene loss can happen by accumulation of loss-of-function mutations through genetic drift [3–5]. Fundamentally, both of these processes are driven by adaptive evolution, whereby beneficial mutations are selected for and deleterious ones removed from the gene pool, ultimately leading to phenotypic diversification [6]. More concretely, trends in the evolution of coding genes can be studied by measuring the ratio of non-synonymous (dN) to synonymous (dS) amino acid rates in the comparison to closely related sequences, usually represented as ω [7]. A ratio higher than one ($dN/dS = \omega > 1$) implies positive selection and thus functional diversification, while a ratio lower than one ($dN/dS = \omega < 1$) indicates the presence of purifying selection and thus a tighter constraint for the diversification of the gene sequence. Most genes in an organism are under strong purifying selection, as a change in a key amino acid of a protein would have a detrimental effect [8]. However, a small portion of them, those that have been subject to recent diversification, show signs of an increased nonsynonymous mutation rate. Codon models that take into account statistical rate variations are commonly used in comparative genomic studies [9]. When performed on related organisms that have different lifestyles and hosts, the study of positively selected genes together with their functional annotation illustrates which gene functions played important roles in the adaptation process.

Oomycetes are eukaryotic organisms belonging, together with diatoms and brown algae, to the group of stramenopiles [10,11]. Since their origin from a marine autotrophic common ancestor around 400 million years ago, oomycetes have adapted to multiple environments and lifestyles, and many of them are economically impactful plant and animal parasites [12–14]. Therefore, they represent a relevant and appropriate system to study the genetic impact of lifestyle and host adaptation on genetically close genomes. Four phylogenetic families, representative of oomycete's large diversity, are the target of most current research efforts: Albuginaceae, Peronosporaceae, Saprolegniaceae, and Pythiaceae. The Albuginaceae and most Peronosporaceae independently evolved the ability to survive exclusively on living host material, also known as obligate biotrophy [15]. However, some Peronosporaceae, particularly in the *Phytophthora* genus, are hemibiotrophs, i.e., they display an initial biotrophic phase followed by a necrotrophic one, during which they feed on the decaying living matter of their host [16]. Additionally in the Peronosporaceae, the early divergent clade of *Globisporangium* consists of plant necrotrophs previously classified as *Pythiaceae*. All Albuginaceae, Peronosporaceae, and most Pythiaceae are plant parasitic organisms [17]. On the contrary, most Saprolegniaceae are capable of infecting animals, with few exceptions including plant-causing root rot *Aphanomyces* and the free-living saprophyte *Thraustotheca clavata*, which does not need a host at any point in its life cycle [18–20].

Obligate biotrophs have a considerably reduced primary metabolism. Comparative genome studies have reported a significant and convergent loss of the enzymatic arsenal in independent lineages of the oomycetes following this lifestyle [21]. The picture is not so clear for the heterotrophs and their adaptation to different hosts. *Pythium insidiosum*, a mammal parasite responsible for pythiosis, shows a relatively recent divergence from *Pythium aphanidermatum* and *Pythium arrhenomanes*, both of which are plant pathogens [22]. There are many theories that explain how such drastic host shifts can occur in a small evolutionary timescale [23]. Particularly in oomycetes, large reservoirs of noncoding DNA material can readily evolve into small secreted proteins, known as effectors, facilitating new oomycete–host interactions [24]. Additionally, the readiness to take up genetic material through horizontal gene transfer from fungi and bacteria has been reported at multiple time points in the oomycete lineages [25–27]. However, the impact of host shifts on genomic selective pressures has not been extensively studied.

There is a high degree of convergent evolution between oomycetes and fungi [28]. Both share many of the niches mentioned, including pathogenic niches of animals and plants, as well as lifestyles, including saprotrophy, hemibiotrophy, and obligate biotrophy. Oomycetes and fungi have developed similar strategies to overcome the same challenges, including comparable filamentous and reproductive morphology, as well as akin infection strategies [29]. As mentioned above, convergence is probably promoted by genetic exchange, as the source of many oomycete genes with a role in host adaptation can be traced back to pathogenic fungi [30]. Because of the parallels between the adaptive strategies of these two eukaryotic phyla, we can infer underlying mechanistic principles in oomycetes on the basis of those further characterized in fungi.

How genome information relates to lifestyle and host adaptation is one of the big questions in ecology, and may be relevant to predict the appearance of new emerging diseases. Understanding the genome characteristics and selective pressures in organisms that have undergone host and niche shifts may offer insights into this question. In this study, we report the first whole-genome positive selection screening of the proteome of the oomycetes phylum, including 34 representative members and an outgroup of eight non-oomycete stramenopiles described in Appendix A. We compared the genes inferred as being under positive selection to the background annotated genes to identify enriched biological functions that may correlate to their adaption to different hosts and lifestyles. Additionally, we developed a method to predict plant pathogenic lifestyle with high accuracy from the genome of fungi and oomycetes, based on the presence or absence of key annotated functions.

2. Materials and Methods

2.1. Data Selection and Functional Annotation

We downloaded stramenopile genetic data from the NCBI and FungiDB databases setting as cutoff assemblies with reported gene annotation, resulting in a dataset of 42 total proteomes. We screened the genomes using BUSCO for high abundance of key orthologs in the stramenopile dataset as a form of quality control [31]. We performed functional annotation of the proteomes using InterProScan version 5.50–84.0 [32]. We validated proteins discussed in the manuscript through comparison with matches from the NCBI datatabase using BLAST [33]. We annotated the effectors in the stramenopile dataset by predicting the secretion signal using the tool SignalP 5.0b followed by an annotation with the model EffectorO [34,35]. We annotated the presence/absence of functional annotations from each genome with the Genome Properties database, performed the clustering with the Python library SciPy and visualized it with the package Seaborn [36,37]. We compared Unweighted Pair Group Method with Arithmetic Mean (UPGMA) clusterings of the genome properties and genome properties with added positive selection information to the phylogenetic tree using the Robison–Foulds metric based on clusters with the application TreeCmp [38,39].

2.2. Phylogeny Inference

We constructed the concatenated stramenopile tree using IQ-TREE 2 with automated partitioned model selection on inferred one-to-one orthogroups present in at least 25 of the taxa in the dataset [40]. We assessed full branch support in all nodes of the phylogenetic tree with 1,000 ultrafast bootstrap repetitions using the IQ-TREE 2 software and displayed it rooted on the outgroup of non-oomycetal stramenopiles.

2.3. Orthogroup Classification and Positive Selection Analyses

We developed a pipeline for whole genome positive selection analysis in Python using the Snakemake modular workflow framework [41]. It uses as input the coding nucleotide sequences as well as their corresponding predicted proteins from each proteome. The code and documentation are available at https://github.com/danielzmbp/wsgups (accessed on 24 June 2021). The steps of the pipeline include: grouping of sequences into ortholog families, their alignment with MAFFT, phylogenetic tree inference using FastTree, codon alignment using PAL2NAL, and finally two positive selection algorithms from the HYPHY package [42–44]. The first step, consisting of the classification of these proteomes into ortholog groups was performed with the software Proteinortho version 6, using the synteny parameter and the Diamond algorithm for homology search [45]. The first HYPHY algorithm used in the pipeline is FUBAR, a site-based program that scans the alignment for pervasive positive selection [46]. Families with at least one codon position under positive selection were subsequently analyzed on all branches with the aBSREL algorithm to relate selective pressures to specific lineages [47]. Taxa downstream of nodes with a corrected *p* value of less than 0.05 were considered under positive selection for this particular gene.

2.4. Enrichment Analyses

We used the Gene Ontology (GO) released in 1 February 2021 [48,49]. We performed GO enrichment using the Python package Goatools based on the InterPro database annotations [50,51]. The background dataset corresponded to the sum of all proteome annotations for the corresponding taxa and the study dataset to the genes found to be under selection. Terms that did not have representative sequences in all analyzed taxa were filtered out. We used as a significance cutoff the negative base 10 logarithm of Holm–Bonferroni corrected *p* values that were higher than 1.3 (*p* value < 0.05). Broad and non-informative GO terms like biological or cellular processes were not included in the enrichment tables.

2.5. Machine Learning Model

The multilayered deep learning models were constructed using the Tensorflow version 2.3 library with the Keras application programming interface [52]. The dataset consisted

of 324 proteomes from fungi and oomycete plant pathogens as well as saprobes. We labeled each proteome as one of the four respective plant pathogenic classes based on the literature consensus: saprotroph, necrotroph, hemibiotroph and biotroph. For the genome properties model, we extracted the features of each genome and encoded them based on the presence or absence of all the identified pathways, which resulted in an array of 5024 binary features each. Removal of duplicated entries resulted in 319 unique samples. For the Carbohydrate-Active enZyme (CAZyme) model, we annotated the proteomes using the db-CAN2 database and encoded the absence or abundance of annotated CAZymes that were identified with the three implemented methods: HMMER, DIAMOND and Hotpep [53]. After removal of duplicates, 313 samples of 593 features were used for training and testing of the model. In both models, we performed a stratified split of the dataset into the training dataset, corresponding to 60% of the total, and the optimization and validation datasets, each corresponding to half of the remaining 40%. Hyperparameter optimization, namely of the learning rate, activating functions and dense layer units, was carried out using Keras Tuner and its implementation of the Hyperband algorithm [54,55].

3. Results

3.1. Proteome Annotation and Clustering

We downloaded the genomes of 34 oomycete species and eight non-oomycete stramenopiles from the NCBI and FungiDB databases and annotated their proteomes by the presence or absence of known functional signatures to gain insights into the divergence of the dataset (Figure 1) [56,57]. The UPGMA clustering based on the Euclidean distance along with midpoint rooting resulted in two main groups, one corresponding to the oomycetes and the other to the remaining stramenopiles. The main difference among them was the lack of photosynthesis-related annotations in the oomycetes, such as chlorophyll biosynthesis (Figure S1). In the oomycetes, we defined three clusters based on their distance (1–3 in Figure 1): obligate biotrophs, Saprolegniaceae, and a final one grouping most of the Perosporanaceae and Pythiaceae of the dataset. The obligate biotroph cluster consisted of the Albuginaceae and the downy mildews from the Peronosporaceae (*Bremia lactucae*, *Plasmopara halstedii*, *Peronospora effusa* and *Hyalopernospora arabidopsidis*). The most striking characteristic was an overall reduction in their metabolism, evident by the lack of many functional annotations in comparison with other oomycetes. This lack of core biosynthetic pathways, including vitamin and cofactor biosynthesis, makes them reliant on their host for growth and survival (Figure S1). The Saprolegniaceae group differed from other oomycetes mainly in the presence of steroid biosynthesis pathways (Figure S2). In the third cluster, we defined two subclusters, labeled as 3.1 and 3.2 in Figure 1. The first contained four of the *Pythium* and *Globisporangium* species of the dataset, and the second one included exclusively all *Phythophthora* in the dataset (except for *Phytophthora megakarya*). The *Pythium* and *Globisporangium* species in the dataset also had biosynthetic pathways that most other oomycetes lacked and that they often shared with the Saprolegniaceae, as a result most likely of their common facultative lifestyles. The hemibiotroph group, consisting of most of the *Phytophthora* species in the dataset, showed significant metabolic reduction, but not as extensive as in the obligate biotrophs [58].

These clusters and subclusters roughly reflected the lifestyles of the taxa in the dataset, mostly highlighted by the hemibiotrophs and obligate biotrophs. To a lesser extent, this was evident in the other two groups as most Saprolegniaceae in the dataset are facultative animal necrotrophs, and most *Pythium* and *Globisporangium* species facultative plant necrotrophs. Interestingly, *T. clavata*, the free-living organism in the dataset, clustered as an outgroup of the other phylogenetically close Saprolegniaceae, showing the greatest distance to its animal and plant-infecting neighbours. The most notable differences in the presence/absence of cellular pathways of this *T. clavata* assembly when compared to other Saprolegniaceae were the absence of the endopeptidase ClpXP complex and RuvB-like helicase I (Figure S2). However, there were some exceptions to this arrangement, with some taxa clustering with a different lifestyle or failing to cluster with their own lifestyle. For

example, the clustering of the two plant infecting necrotrophs of the Saprolegniaceae follows the phylogeny of the *Aphanomyces* genus. Additionally, *Globisporangium splendes* appears as an outgroup of group 3.1 despite having a similar plant necrotrophic lifestyle and being phylogenetically closely related to other members in this clade (Figure S3). An explanation for this could be its long-read sequencing-based assembly. Long-read sequencing technology has been shown to produce much larger genomes in oomycetes when compared to the classical short-read sequencing, as hard-to-assemble repeat-rich regions are a common feature of their genomes [59]. However, other long-read assemblies in the dataset (*B. lactucae*, *Saprolegnia parasitica*, *Phytopythium vexans* and *Phytophthora fragariae*) show no apparent influence in the clustering (Figure 1).
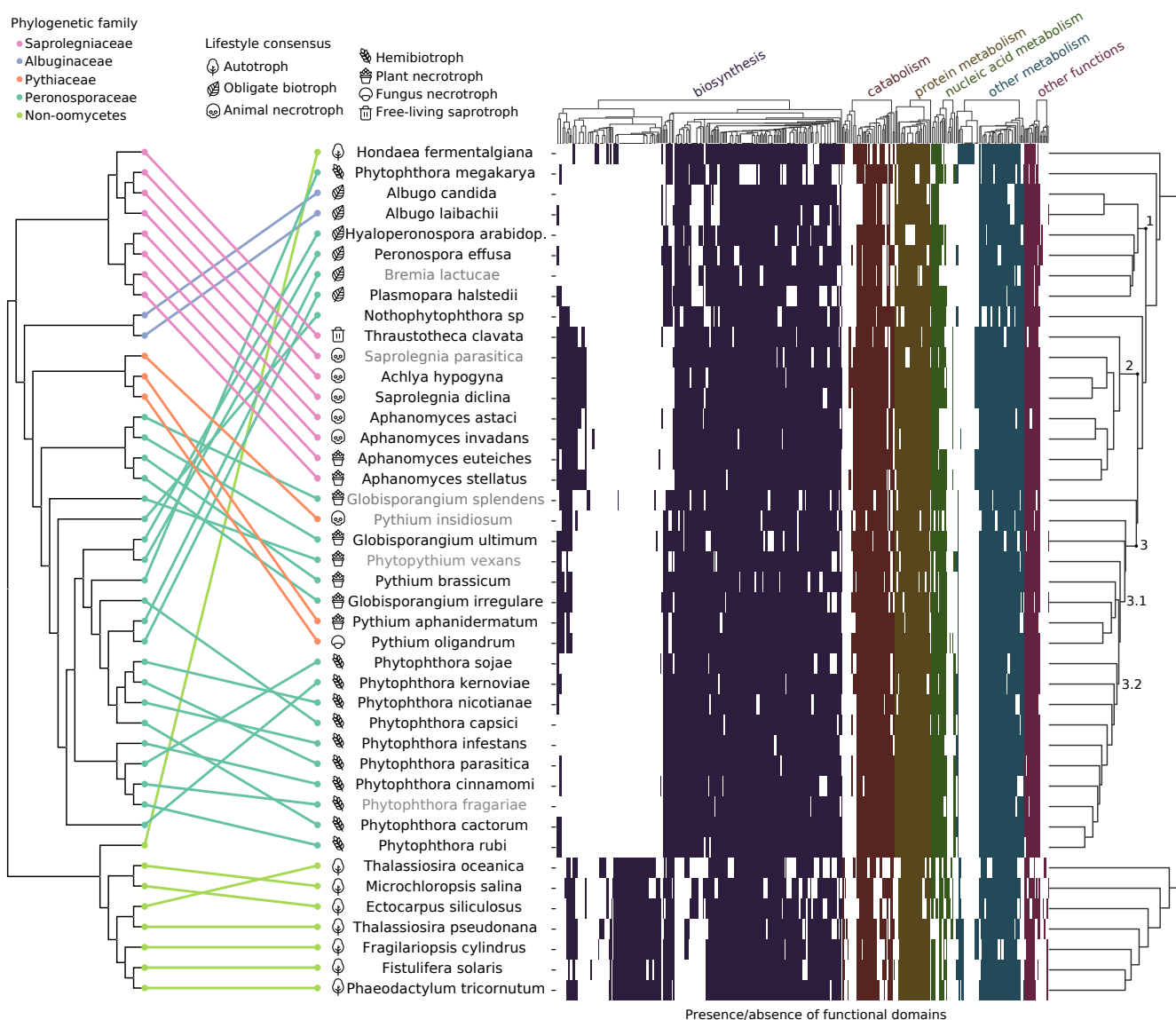

Figure 1. Presence/absence of functional attributes in the genomes of the stramenopile dataset correlated with phylogeny. Equal distance cladogram constructed from conserved families inferred by the maximum likelihood on the left and clustering by Unweighted Pair Group Method with Arithmetic Mean (UPGMA) of genome properties of the dataset on the right. In the equal distance phylogenetic tree, colored lines match phylogeny to the clustered taxa with annotated lifestyles. All nodes in the tree have a 100-bootstrap support. In the heatmap, different colors represent the presence or absence of particular functional groups belonging to the specified categories. Names in grey represent long-read sequencing assemblies in the dataset for that species.

3.2. Ortholog Group Classification

To infer positive selection from the stramenopile dataset of 42 genomes, we classified the proteomes into ortholog groups by taking sequence similarity and in addition gene order into account. We selected protein clusters that had at least five members from different taxa to obtain a good balance between a representative number of families and results that are statistically robust. This corresponded to 29,123 protein families, which cover about half (49.02%) of the total proteins in the dataset (Figure 2a). The orthogroups were mainly composed of one-to-one orthologs (78.70% of families); however, we detected a significant number of paralogs in some oomycetes, particularly for *Nothophytophthora* sp., as well as for *Phytophthora nicotianae*, *G. splendens* and *Phytophthora parasitica* (Figure 2b). This might be related to the reported whole genome duplications in *Phytopthora* species [60], as well as the recent hybridization event that gave rise to *Nothophytophthora* [61]. Additionally, the diatom *Fistulifera solaris*'s large presence of gene duplications highlights its recent whole genome duplication [62]. The larger presence of duplicates in *P. insidiosum* and *G. splendes* in comparison to their peers may originate from their long-read sequencing-based assembly, which is better able to resolve gene duplications.

The most abundant orthogroups had between five and nine members (Figure 2c). Orthogroups corresponding to all taxa were a minority. Instead, most orthogroups were present in closely related five- to ten-member clades. When looking at the number of genes not assigned to orthogroups in the oomycetes, the *Phytophthora* genus had the highest count (Figure 2a). This may be related to the large arsenal of unique effectors that lack conserved domains or homologs outside of their own species and play a large role in host adaptation. *Aphanomyces astaci* also had a high amount of genes outside of the orthogroups, most likely because of the recent expansions in its genome [63]. In summary, this highlights a patchy ortholog distribution in the dataset, with most protein families conserved only in phylogenetically close members of clades (Figure 2c). Despite this, a significant pool of ortholog protein families representative of the stramenopile genomes in the dataset could be inferred from the analysis as further discussed below.

3.3. Positive Selection Analyses

Positive selection screening for orthologous groups was performed by using first a site-specific codon model to detect families under selection. This was followed by a branch-site-specific codon model to detect the taxa experiencing positive selection on those genes. The number of genes under selection varied for the different phylogenetic clades. Members of the Saprolegniaceae and Pythiaceae, together with the necrotrophic *Globisporangium* had a higher count and therefore more genes under selection in orthogroups (mean = 1222, std = 152) than the remaining Peronosporaceae and the Albuginaceae (mean= 577, std = 245) (Figure S5). A special case was the hybrid *Nothophytophthora* sp., which had a comparable amount of positively selected genes to Pythiaceae and Saprolegniaceae, however, composed in great part by duplicated genes after speciation, 44.45% of the total (orange bar). When comparing necrotrophs, hemibiotrophs, and obligate biotrophs within the Peronosporaceae family (mean = 1344, 663, and 269, respectively), the trend was that of a decrease in the number of genes under positive selection with the increase in biotrophic potential (Figure 3).

To infer potential biases in our analyses, we tested for a correlation between the number of genes under positive selection and the amount of proteins classified into orthogroups for each taxa (Pearson's correlation, r = 0.50, *p* value < 0.01). A correlation of 0.5 suggested that there may be a larger number of positives because of more extensive testing in the oomycete species, as they have on average more members in the ortholog dataset. This bias is more evident in the non-oomycetes (Pearson's correlation, r = 0.52, *p* value = 0.18) than when considering just the oomycetes (Pearson's correlation, r = 0.15, *p* value = 0.39). As the proteomes of the non-oomycetes are overall smaller compared to oomycetes (Figure S4), we hypothesize that less extensive testing renders them more prone to this bias.
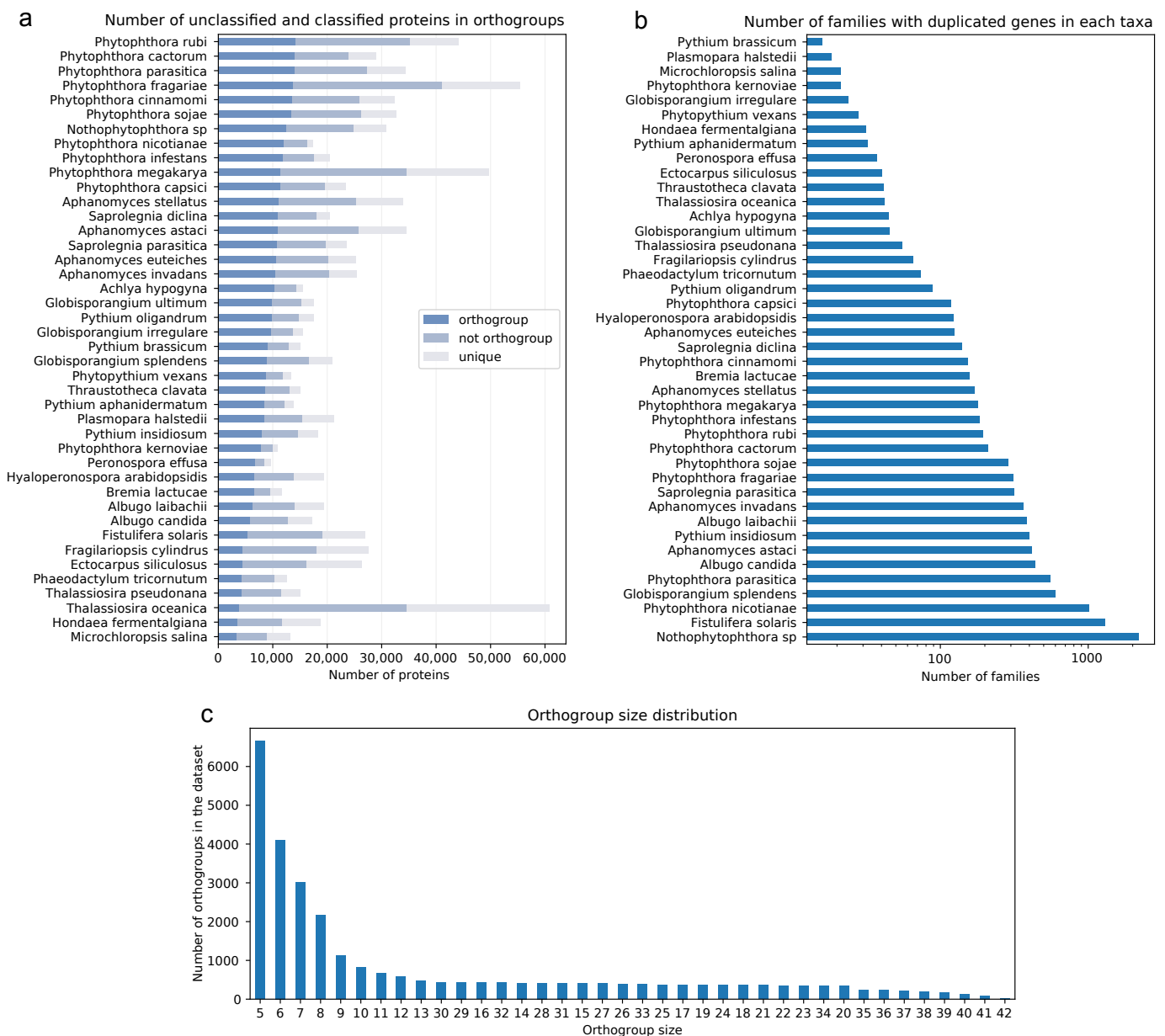
Figure 2. Orthogroup classification in the stramenopile dataset. (**a**) Protein-encoding genes from the dataset grouped into ortholog families. Number of genes classified into orthogroups (protein families of five or more members), not classified into orthogroups (protein families of less than five members), or unique (not in a protein family) are displayed per taxa. (**b**) Duplicates in protein families of the dataset. Number of ortholog families with five or more members from different taxa that contain paralogs (two or more genes from the same taxa). (**c**) Distribution of protein family size in the dataset. Number of families with the same member size are represented as a histogram.

Out of the 32,661 detected genes under positive selection, 21,247 were successfully annotated with at least a GO term (65%). We performed GO enrichment on the four main oomycete lifestyles in the stramenopile dataset. The results are discussed below. As a control for the reliability of the pipeline, we performed the same analyses in a subset of 26 plant pathogens from a dataset of 65 basidiomycete fungi (Table S1). Highly enriched terms included processes known to be associated with virulence in such pathogenic fungi, like fatty acid and certain amino acid biosynthesis, ion transport, and protein targeting and transport (Table S3) [64–66].

In summary, we could identify signatures of positive selection in 4.14% of all genes analyzed in the stramenopile dataset. A significant number could be functionally annotated and potential functions assigned.
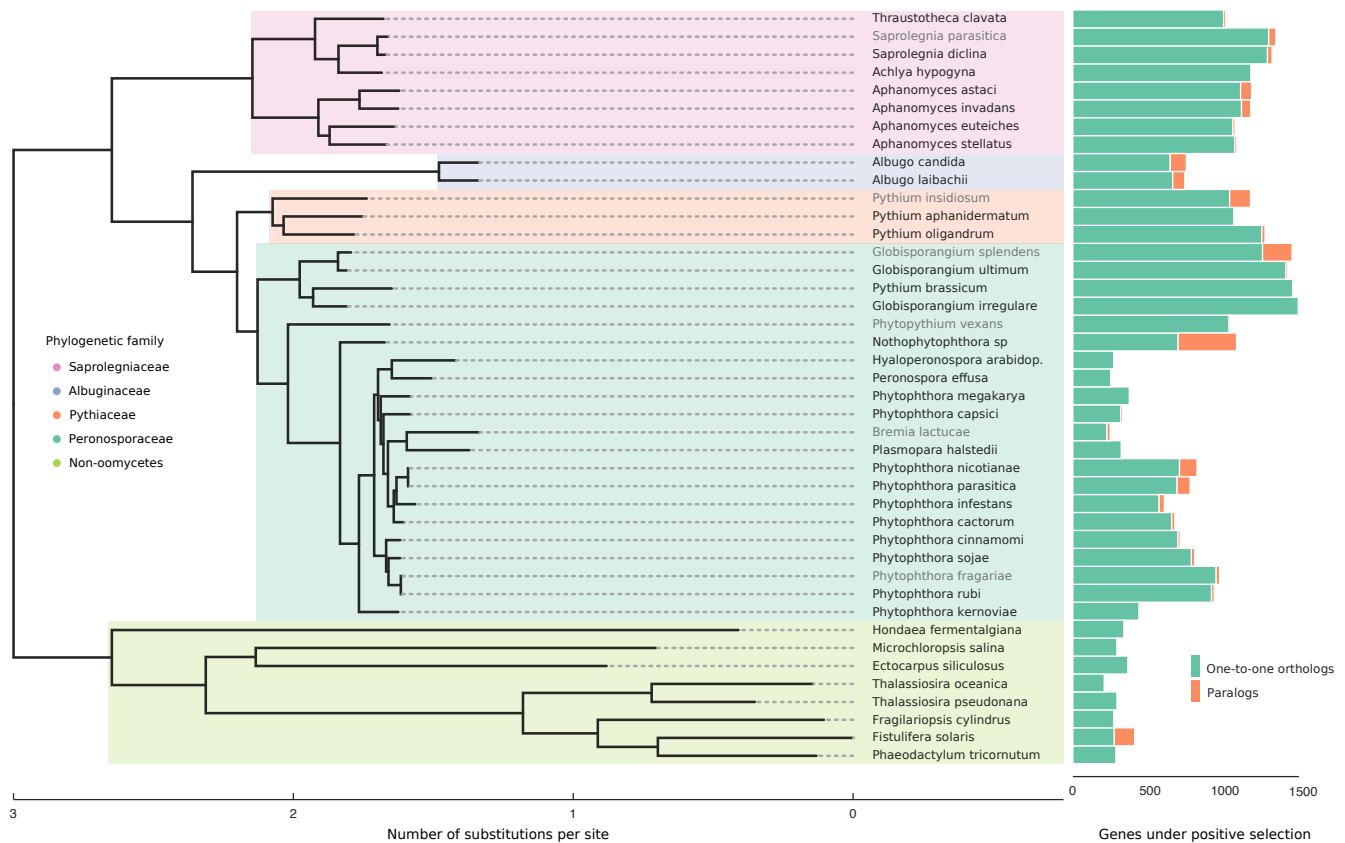

Figure 3. Number of genes under positive selection in the stramenopile dataset. The Maximum likelihood supertree with 100-bootstrap support in all nodes was constructed from inferred protein families in the stramenopile dataset that are conserved in at least 25 taxa, corresponding to 3013 families of orthologs. A number of positively selected genes are represented as bars. One-to-one orthologs are in green, duplicated genes inside the same family under positive selection in orange. Names in grey represent long-read sequencing assemblies in the dataset for that species.

3.4. Enriched Biological Functions under Selection

To gauge the selective pressures for adaptation to a parasitic lifestyle in the oomycetes, we explored the enriched GO terms that were pervasive in all oomycetes (Figure 4a). Highly enriched term categories related to response to stress, signal transduction, transmembrane transport, protein modification processes (phosphorylation, in particular), and localization, as well as numerous carbohydrate, lipid, nitrogen, and sulfur metabolism-related terms. Within the metabolism, abundant terms relating to biosynthesis are present. In the cellular compartment GO category, highly enriched terms include protein-containing complexes (for which transferase complexes show the larger significance), nucleus, intracellular organelles (for which ribosome shows the largest significance), and membranes (Figure 4b).

Additionally, we performed similar enrichments on the oomycete groups as defined by their lifestyle. We found the largest amount of unique GO terms to belong to the plant and animal necrotrophs (36 and 21, respectively). In the plant necrotrophs, these included terms related to ion transport, carbohydrate biosynthesis, protein modification, and gene expression regulation. In the animal necrotrophs, unique terms had to do with vitamin biosynthesis, cilium movement, and protein localization. There were three unique terms in the hemibiotrophs related to response against stress and transmembrane transport while no unique terms were identified in the obligate biotrophs. We observed the largest overlap between animal and plant facultative necrotroph groups (59 common terms). These terms

related to cell communication, glycolysis, organelle assembly, protein import, regulation of response to stimulus, translation, and numerous and diverse metabolic processes. This was followed by a smaller overlap of enriched functions in all four lifestyle groups, amounting to 33 terms (Figure 4c). The significant terms for each lifestyle are all listed in Tables S4–S9.
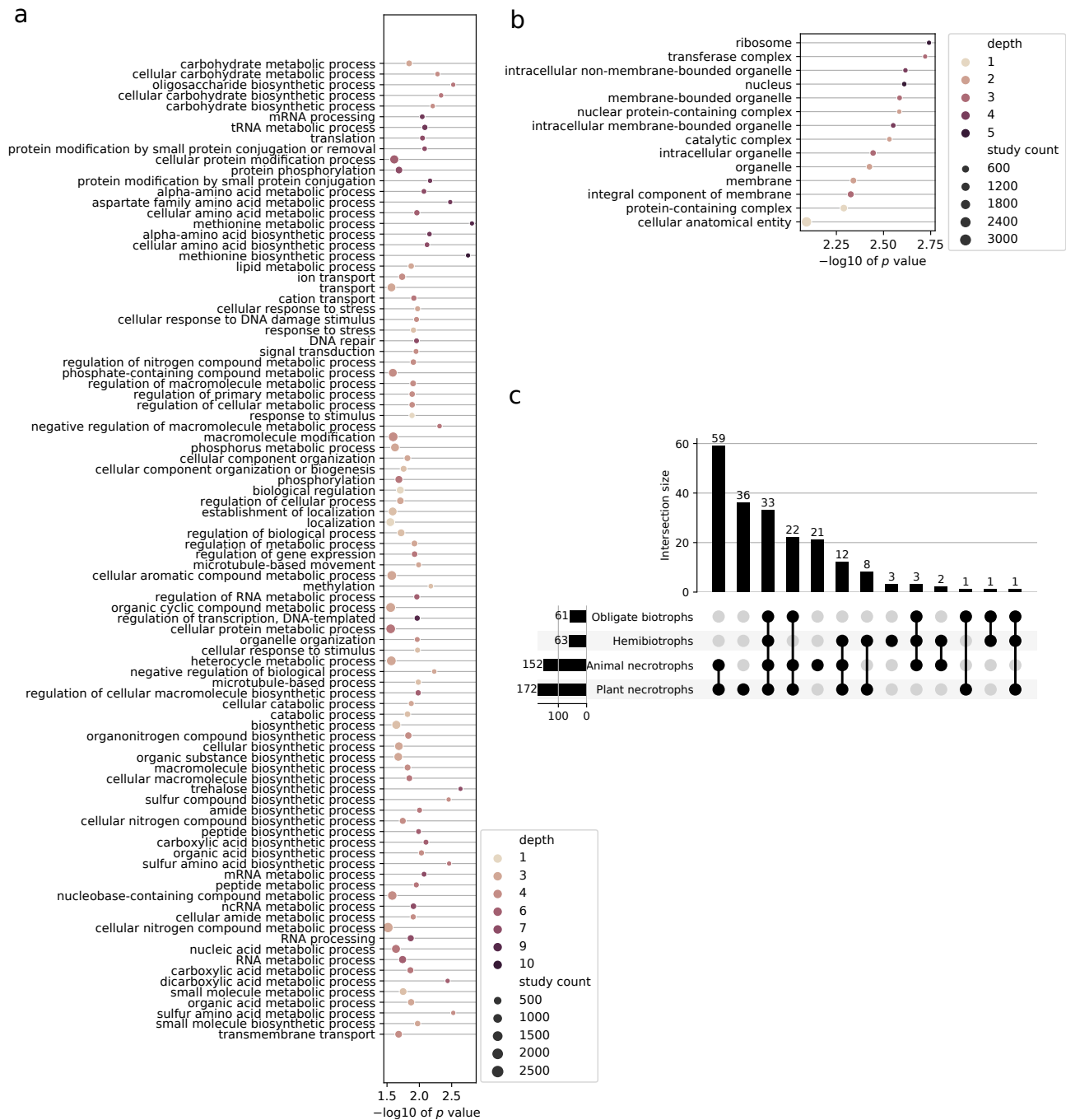

Figure 4. Functional and location enrichment of positively selected genes in the oomycetes. Significantly enriched (**a**) biological processes and (**b**) cellular compartments in all oomycetes that show signals of positive selection in the stramenopile dataset. Included are gene ontology (GO) terms with a corrected negative base 10 logarithm of the *p* value higher than 1.5 ordered by category using the GO slim database. The color represents the GO depth. GO depth is a measure of the number of parent nodes in the GO tree. That is, the more specific the GO term, the higher its depth. The size of the dots corresponds to the total number of proteins under selection in the stramenopile dataset that belong to said term. (**c**) Upset plot showing number of overlapping biological functions under selection in the oomycetes. The four groups correspond to the major lifestyles in the oomycetes of the stramenopile dataset.

We also studied the enrichment of biological functions in the expanded gene families of the dataset independently of whether the genes were under positive selection. In general, we found that it reflected positive selection enrichment; however, the terms were highly variable when comparing different species (Table S10). In the obligate biotrophs, these related to phospholipid metabolism, cell wall biosynthesis, protein modification, biological regulation, and transmembrane transport. In the hemibiotrophs, they related to lipid metabolism, signaling, protein modification, and again to biological regulation, and transmembrane transport. Finally, in the plant necrotrophs, they related to DNA integration and localization.

3.5. Lifestyle Prediction

We visualized in a heatmap all functional annotations with added information of positive selection by performing the same clustering as we did for the genome properties (Figure 5). We find that adding the positive selection data improves the clustering by lifestyle, particularly of the plant necrotrophs in the Pythiaceae and *Globisporangium*, which now form a single cluster that is closer to the other facultative necrotrophs of the dataset, the Saprolegniales, than to the obligate biotroph and hemibiotroph oomycetes in the dataset. Using the Robison–Foulds metric for clusters, we observed that there is a higher congruence between the phylogenetic tree and the genome properties clustering than to the positive selection one (Table 1).
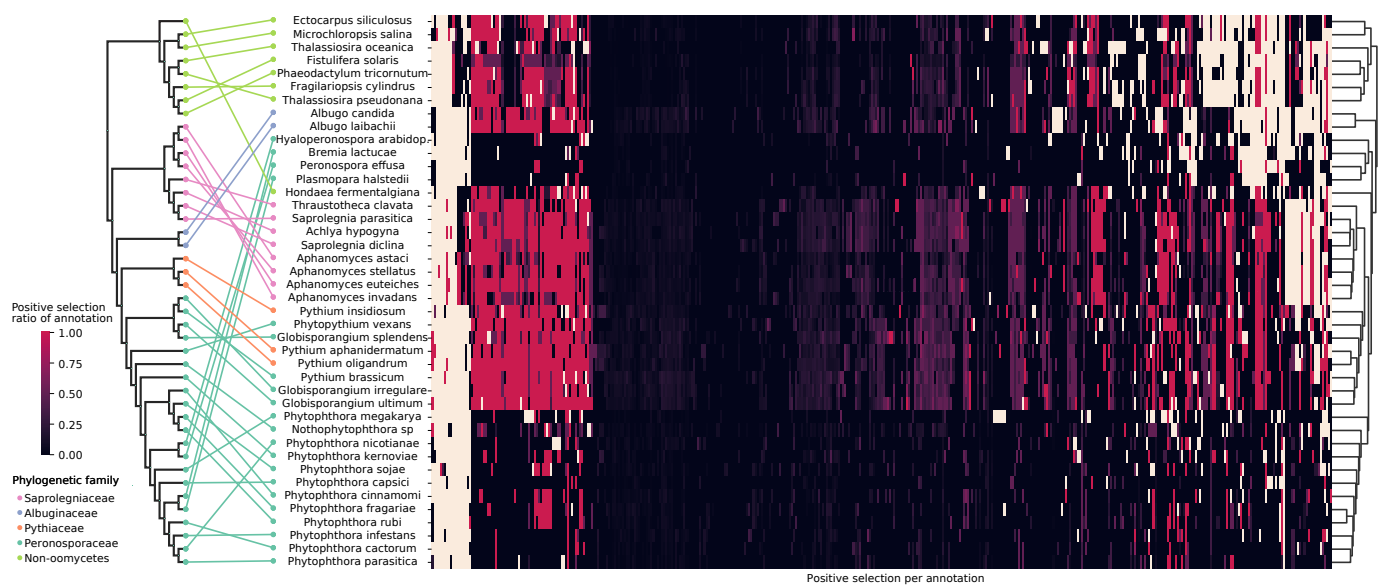

Figure 5. Heatmap of positive selection ratio of functional annotations in the stramenopile dataset. The color gradient from black to red in the heatmap represents the ratio of genes with a particular functional annotation that are under selection. Cream-colored cells represent the absence of the annotation for that species. The phylogenetic equal distance cladogram is represented on the left while UPGMA-based clustering of the distance between the taxa is represented on the right. Colored lines representing the phylogenetic family connect both clusterings.

Although positive selection information improved lifestyle clustering, we argue that it is impractical to implement as a prediction method because of its computationally demanding calculation and poor reproducibility when using different backgrounds for positive selection analyses. Therefore, we constructed a model to predict lifestyle in plant pathogenic fungi and oomycetes based on the genome properties alone. We assembled a dataset comprising 324 genomes from 115 plant pathogenic and saprotrophic fungal and oomycetal species (Table S2). We used the annoted genome properties as features to build a deep neural network classifier with four output classes corresponding to their lifestyle consensus in the literature: saprotroph, necrotroph, hemibiotroph and biotroph. We found a high accuracy on the validation dataset for the optimized model (loss = 0.11,

accuracy = 0.95), failing to predict two genomes in the hemibiotrophs and one in the biotrophs of the validation dataset (Figure 6). For comparison with published models, we additionally constructed a predictor based on Carbohydrate-Active enZymes (CAZymes), which also resulted in a high accuracy for the random validation dataset and performed better in the prediction of hemibiotrophs (loss = 0.14, accuracy = 0.97). Both models and the steps to reproduce them together with the entire dataset can be found at https: //github.com/danielzmbp/lspred (accessed on 24 June 2021).

Table 1. Distance comparisons in the clusterings of the stramenopile dataset. Phylogenetic and genome properties clustering is shown in Figure 1 and positive selection clustering in Figure 5.

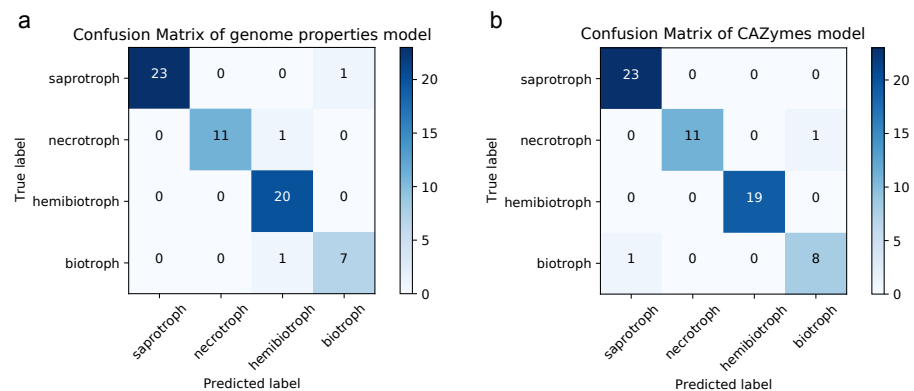| Clustering 1	Clustering 2	Robison–Foulds Distance Metric
Phylogenetic	Genome properties	28
Phylogenetic	Positive selection	30
Genome properties	Positive selection	24

Figure 6. Confusion matrix of lifestyle predictor models. Prediction results in the random validation sets for the constructed models based on (**a**) genome properties and (**b**) Carbohydrate-Active enZymes (CAZymes), corresponding to 64 and 63 annotated proteomes, respectively (20% of the total dataset). True values are represented on the *x*-axis and predicted values on the *y*-axis.

4. Discussion

4.1. Functional Genome Annotations Largely Correlate with Lifestyle

Convergence of the presence/absence of key functional annotations in species that do not share the same phylogenetic history but have similar lifestyles has been shown before for different sets of organisms [67,68]. Distant species with the same lifestyle require similar functional biological processes, which results in similar selective pressures that analogously shape their genome, often leading to convergent evolution. Comparable to the study by Rodenburg et al. (2020) [69], we have shown the tight clustering of some oomycete groups with a similar lifestyle, most strikingly for the obligate biotrophs and hemibiotrophs. Conversely, we find a few exceptions in our dataset, such as the hemibiotroph *P. megakarya* and the necrotroph *G. splendens*, which do not clearly cluster with any of the other oomycetes. We hypothesize this may be partly due to the quality of their gene annotation. Both have a significantly lower number of complete key orthologs than the reference stramenopile BUSCO database as compared to other *Phytophthora* and *Globisporangium* species in the dataset (Table A1).

4.2. Generalists Have More Genes under Positive Selection

A higher number of genes under selection was found for the more generalist families of Saprolegniaceae, Pythiaceae, and necrotrophic Peronosporaceae, including the *Globisporangium* and *Phytopythium* clades, when compared to the higher number of specialists remaining in Peronosporaceae and Albuginaceae (Mann–Whitney test, $p < 0.01$). Within the Peronosporaceae, hemibiotrophs have a lower number of genes under selection than the facultative necrotrophs, and obligate biotrophs have in turn a lower number than hemibiotrophs (ANOVA one-tailed test, $p < 0.01$) (Figure S5). Thus, the number of genes under selection is inversely correlated to the biotrophic potential. With biotrophic potential, we refer to the capability of the pathogen to survive exclusively on a living host, such that no obligate biotroph can be cultured in vitro, while for some hemibiotrophs this is the case. On the opposite side of the spectrum, facultative plant necrotrophs thrive as saprotrophs without the need for a host. This correlation cannot be explained alone by the different sizes of the proteomes in the dataset or by their phylogenetic closeness (Figure S4). However, we hypothesize that both of these factors confound our results to a large extent. Smaller proteomes in the dataset, as is the case of the non-oomycetes, show a larger correlation of their size to the number of genes under positive selection. The phylogeny influence is highlighted by the similar number of genes under positive selection of taxa within the same genus as shown in Figure S4.

While all hemibiotrophs and biotrophs are obligate plant parasites, the necrotrophs in the Peronosporacea, Pythiaceae and Saprolegniaceae families show adaptation to a variety of lifestyles. They are facultative parasites of either animals, plants, or other fungi and oomycetes. Facultative parasites can live as saprotrophs on decaying matter but also as opportunistic necrotrophs on a suitable host [70]. The higher number of potential niches they are able to successfully occupy may drive a larger number of genes to be under positive diversifying selection. Additionally, when compared to the obligate biotrophs and hemibiotrophs, which are highly adapted to infect a particular species, e.g., lettuce for *B. lactucae* and soybean for *Phytophthora sojae*, most of the necrotrophs are able to infect a wide range of hosts. For instance, *A. astaci* is capable of infecting up to twelve genera of crayfish and is known for its ease of host jumping [71]. Having a higher number of genes under positive selection could be therefore correlated with this higher host flexibility.

4.3. Selective Pressures in the Ooomycetes Help Explain Host Adaptation

Biological functions under selection for all oomycetes in the stramenopile dataset, shown in Figure 4, give insight into which of these are important for the diversification in this clade. Many biosynthetic functions, particularly related to carbohydrates, are found to be enriched. Different cell wall carbohydrate composition has been found for different clades in the oomycetes, likely associated to different lifestyles [72]. Lipid metabolism, known also to be important for host adaptation in plant pathogenic fungi and oomycetes, is also enriched [73]. Transport-related proteins, and in particular cation transport, are also prominently enriched in these terms. As an example, the role of the expanded calcium transporter genes in the oomycetes has been extensively studied in the context of host interaction [74]. Overall, many of these terms allude to important virulence factors known for the oomycetes: transmembrane transport, effector protein processing and secretion, cell wall synthesis and remodeling, and lipid localization [75].

4.3.1. Selective Pressures Relate to Lifestyles in Oomycetes

The enriched terms common to the Albuginaceae and downy mildews greatly relate to known virulence factors for these plant pathogens, including carbohydrate metabolism, protein modification, transport, negative regulation of gene expression, and response to stimuli (Table S4). This suggests that these biological functions are under selection and played a big role in the adaptation of oomycetes to an obligate biotrophic lifestyle. Some of these, particularly carbohydrate metabolism, transport, and protein modification,

are common to the other plant pathogens in the hemibiotrophs and plant necrotrophs (Tables S5–S7), highlighting a broader mechanism of adaptation to a plant-parasitic lifestyle.

One of the most often found terms and among the most enriched in both the obligate biotrophs and the hemibiotrophs of the dataset corresponds to regulation of biosynthetic and metabolic processes, and particularly negative regulation. This may underscore the fitness advantage for rapid growth during the hyphal stage and its need for activation or deactivation according to the circumstances. When the hyphal stage takes place after colonization, the salvaging and biosynthesis of carbohydrates, nucleic acids, and lipids with the resources obtained from the plant host is key for a successful infection. Beta-glucan, for example, is an important component of the oomycete's cell wall and is also an elicitor of the plant immune response [76]. Its biosynthesis features prominently in the enriched terms for the hemibiotrophs. Following the hyphal stage and massive host colonization, there is a reproductive, mainly sporulating stage which needs to be tightly regulated. The latent period between infection and sporulation has been shown recently to correlate to different pathogenic lifestyles in leaf pathogens [77]. A widely diversified family of proteins in the oomycetes that take part in transcriptional activation and help regulate sporulation are Myb transcription factors [78,79]. The ortholog family of the gene *Myb3R7*, which was shown in *P. infestans* to be upregulated during sporulation, shows high rates of positive selection for the *Aphanomyces* and *Pythium* clades. Another gene associated to sporulation, classified as *CDC5*, was also found to be under selection in the oomycetes of the stramenopile dataset.

Secretion of small effector proteins, as in other fungal filamentous pathogens, is key for host adaptation in plant pathogenic oomycetes [80]. Many unique effector proteins have been characterized in the oomycetes that contribute to virulence by modulating the immune response of the plant [81]. Therefore, this dependence on the secretion machinery of the cell for successful infection and thus survival has led to high selective pressures on their genome. We observed significant enrichment of the effectors in the positively selected terms in all oomycetes of the dataset (hypergeometric test, $p < 0.01$). When looking at the enrichment per species; the majority of the *Phytophthora* and plant necrotrophs, which significantly depend on effector proteins for host infection, were also enriched (Figure 7a). The obligate biotrophs, which also depend greatly on secreted effectors, do not show enrichment in our analysis. This may be due to the lack of orthologs on host specific effectors and thus not them not being analyzed in the positive selection screen. There is a small correlation between the number of positively selected genes compared to those predicted to be effectors (Pearson's correlation, r = 0.22, p = 0.22), so these results may be slightly skewed due to testing bias (Figure 7b). In the GO enrichment of all oomycetes, there were several processes directly related to protein secretion under selection, including protein modification. Other secretion-related terms, although more general, also showed enrichment, including those relating to microtubule-based processes in the obligate biotrophs, and transmembrane transport in the hemibiotrophs.

Another interesting term indirectly related to effector proteins is sulfur amino acid biosynthesis. This term is highly enriched in the hemibiotrophs and the necrotrophs of the dataset. This may be associated with the abundance of cysteine-rich proteins in the effector arsenal of the plant pathogens with a necrotroph phase [82]. The disulfide bonds that link cysteine residues help maintain the structural integrity of the proteins released into the extracellular space called apoplast, a hostile environment that is slightly acidic and rich in plant proteases [83]. In general, elevated amino acid biosynthesis has been shown to be an important factor during infection of plant hemibiotrophs such as *P. infestans* [84]. We found enzymes related to amino acid biosynthesis, namely methionine synthase and ketol-acid reductoisomerase, to be under pervasive positive selective pressure in most oomycetes in the stramenopile dataset. These were previously found to be upregulated during early infection and the switch to necrotrophic phase in *P. infestans* [84].

When looking exclusively at the necrotroph groups, many terms in the plant pathogens overlap with the animal pathogens, most likely relating to their facultative saprobe lifestyle.

These include glycolysis, generation of energy, cell communication, as well as amino acid, tetrapyrrole, and amide biosynthetic processes. The latter group is most likely enriched as a result of their autotrophic and more developed secondary metabolism compared to that of other oomycetes, which makes them suited to a free-living lifestyle [85]. The highest enriched term under positive selection for both groups corresponds to the inosine salvage pathway, in particular the enzyme inosine 5'-monophosphate-specific 5'-nucleotidase. Nucleoside accumulation in the plant apoplast has been shown to increase susceptibility to the plant fungal necrotroph *Botrytis cinerea* [86]. A similar case in oomycete necrotrophs could have led to high selective pressure on this enzyme. Equally interesting is the term DNA ligation involved in DNA repair, which may be related to the defense against oxidative stress that is key to the immune response in plants and animals against such pathogens [87].
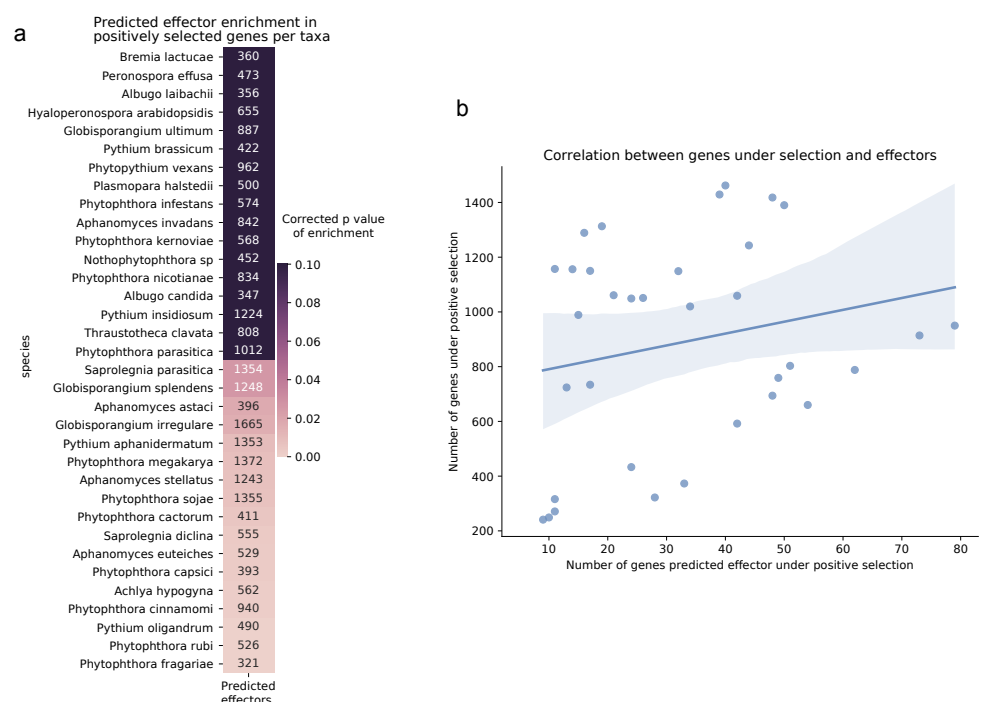

Figure 7. Effector proteins in the oomycetes of the stramenopile dataset. (**a**) Enrichment of genes coding for effector proteins under positive selection in oomycetes. The color gradient represents significant *p* values from hypergeometric tests per taxa corrected for multiple testing using Bonferroni. A lighter shade represents a more significant enrichment. The numbers within the cells represent the total effectors per proteome in the stramenopile dataset that were analyzed for positive selection. (**b**) Correlation between genes under selection and effectors in the oomycetes. Pearson correlation is represented as a straight line and the confidence interval is represented as a lighter shade (r = 0.22, *p* value = 0.22).

4.3.2. Biosynthetic Repertoire Is Important for Lifestyle Adaptation

As shown in Figure 1, the biosynthetic repertoire of each taxa plays a big role in defining the lifestyle of the organisms in the stramenopile dataset. Particularly interesting in oomycetes is the evolutionary history of sterol *de novo* biosynthesis. It is present in Saprolegniales and absent in other oomycete lineages due to their inability to synthesize oxidosqualene [88,89]. The squalene synthase shows hints of positive selection in *Aphanomyces* (Figure S6). Furthermore, positive selection is pervasive in the enzymes that take part in sterol biosynthesis in the stramenopile dataset.

Vitamin biosynthesis as well plays a big role in the evolution of pathogen adaptation to its host. Vitamins are expensive to produce and often require dedicated pathways. Heterotrophs that have adapted to obligate biotrophic lifestyles, such as *Albugo* and the downy mildews, circumvent this by losing their biosynthetic capabilities and developing ways of utilizing host vitamin supply, also known as auxotrophy [90]. Meanwhile, those that live without a host at any point in their lifecycle must maintain these pathways under strong purifying selection. In our dataset we found signatures of positive selection in several enzymes relating to tedrahydrofolate (THF) salvage and biosynthesis, namely dihydrofolate synthase and phosphoribosylglycinamide formyltransferase (Figure S7). As THF is a derivative of Vitamin B9 or folic acid, it is crucial for the synthesis of several amino acids such as serine and methionine as well as for purines and thiamine [91]. It is therefore likely that oomycetes that are not able to obtain THF from a living host have strong selection to maintain THF metabolism in order to ensure their own amino acid biosynthesis.

Molybdopterin cofactor is important for the production of certain detoxification enzymes [92]. In oomycete obligate biotrophs, molybdopterin-related biosynthetic pathways have been lost independently several times in the oomycetes' lineage due to host adaptation [15]. Molybdopterin metabolism was found under high selective pressure in the facultative necrotrophs and autotrophs of the stramenopile dataset, including *Saprolegniaceae* and *Pythiaceae* families, and *Phytophthora* genus (Figure S8). The biosynthesis of molybdopterin cofactor also features as an enriched GO term in the plant necrotrophs (Tables S6 and S7).

Proteins relating to the glycolysis pathway and amino acid biosynthesis have a special evolutionary history in the oomycetes [93]. Many of these enzymes originated from horizontal gene transfer from plants or bacteria. This might explain their high rate of positive selection, which is usually the case for genes recently acquired by horizontal transfer, as they need to be adapted to the new host. In the glycolysis pathway, we detected signatures of positive selection for most oomycetes in the stramenopile dataset, particularly in the enzymes glyceraldehyde-3-phosphate dehydrogenase and fructose-bisphosphate aldolase (Figure S9).

4.3.3. Protein Family Enrichment Reflects Lifestyle Selective Pressures

The large overrepresentation of paralogs as positively selected genes is evident in many of the taxa (Figure 3). After a gene duplication event occurs, there is usually an increase in the selective pressure on one of the copies that maintains the function. Meanwhile, in the other one, these constraints are relaxed, freeing it for potential divergent evolution [94]. Interestingly, many of the enriched functions in the paralogs correlated with terms under positive selection for their specific lifestyle (Table S11). In the *Phytophthora* lineages these include biological regulation, glycolipid biosynthesis, and transmembrane transport. In *Albugo* and other obligate biotrophs, protein modification, carbohydrate metabolism, biological regulation, and glutamine metabolism.

4.4. A Model Based on Genome Properties Accurately Predicts Lifestyle

The genome convergence of phylogenetically diverse fungi and oomycetes allowed us to create a model that can predict plant pathogenic lifestyle based on annotations from both eukaryotes. Assessment of lifestyle from genomic properties in plant pathogens has been traditionally performed by characterizing cell wall-degrading enzyme annotations [95]. To our knowledge, there is only one other published model that attempts to predict lifestyle from genomic features [96]. This model predicts trophic categories based on principal component analysis of CAZyme annotations. We find that our model, which in contrast is based on entire genome annotations, allows for better overall accuracy. However, its better performance may be partly related to its four output lifestyles compared to the seven classes in the model from Hane et al. (2020), since when comparing the genome properties model to a four-class model trained using similar parameters on CAZymes, the prediction is comparably precise (Figure 6). An advantage of the genome properties

model is that having trained it on a larger number of features per sample allows for a more accurate prediction of incompletely annotated specimens that may result from environmental sampling. Given the availability of increasing proteomic and transcriptomic data of unknown fungal and oomycetal origin, such prediction tools will become crucial to identify the pathogenic potential of facultative and obligate parasites.

5. Conclusions

The presence/absence of metabolism-related genes is known to converge for phylogenetically distant organisms that follow the same lifestyle [69,97]. Here, we report a similar case for our dataset of stramenopiles. We developed a pipeline for seamless throughput analysis of positive selective pressures using genome data as input and employed it to show that patterns of selective pressure also converge on hosts that cannot be explained by phylogeny alone. Clustering the taxa by their positive selection predictions, we showed improvement in the prediction of their lifestyle. Furthermore, we identified a number of biological functions that are commonly found under selection for all oomycetes independently of lifestyle. We explored and discussed lifestyle-specific adaptive genes that corresponded to biological regulation, transport, protein modification and metabolite biosynthesis. Finally, we described a model based on genome properties that is able to accurately predict the plant pathogenic lifestyle of filamentous fungi and oomycetes.

Overall, we believe our results highlight to date unexplored genes that could lead to further understanding of lifestyle evolution in oomycetes, and more broadly in filamentous pathogens. Experimental exploration on the impact these adaptations may have in the function and behaviour of the encoded proteins could improve prevention and prophylaxis against new emerging pandemic threats. Particularly, the enzymes reported in this manuscript, due to their likely adaptation as a consequence of a shift in host or lifestyle, may present interesting new targets which could be further explored for disease control.

Supplementary Materials: The following are available online at https://www.mdpi.com/article/10.3390/pathogens10070807/s1, Figure S1: Differences in annotated cellular pathways from the stramenopile dataset. Shown are pathways which have up to 36 repeated values per taxa. The clusters from Table 1 are encapsulated in a labeled square, Figure S2: Differences in annotated cellular pathways for the members of the Saprolegniaceae family in the stramenopile dataset. Shown are pathways which are different in at least one taxa and have at least one complete loss in any of the taxa, Figure S3: Differences in annotated cellular pathways for the members of the Pythiaceae family and *Globisporangium* genus in the stramenopile dataset. Shown are pathways which are different in at least one taxa and have at least one complete loss in any of the taxa, Figure S4: Correlation between genes under positive selection and proteome size in the stramenopile dataset. Oomycetes are in blue (Pearson's correlation, r = 0.15, *p* value = 0.39) and non-oomycetes in red (Pearson's correlation, r = 0.52, *p* value = 0.18). Pearson correlation is represented as a straight line and the confidence interval is represented as a lighter shade, Figure S5: Comparison of the distribution of positive genes under selection for different lifestyles. Significance between the different categories is $p < 0.01$ in both the upper graph (Mann–Whitney test) and the lower graph (ANOVA one-tailed test), Figure S6: Sterol biosynthesis-related enzymes in stramenopiles. Heatmap of the presence and absence of the enzymes relating to the sterol biosynthesis pathway in the stramenopiles. The yellow gradient represents the normalized ratio of the predicted positive selection in genes with this annotation, Figure S7: Tetrahydrofolate salvage and biosynthesis-related enzymes in stramenopiles. Heatmap of the presence and absence of the enzymes relating to tetrahydrofolate metabolism in the stramenopiles. The yellow gradient represents the ratio of predicted positive selection in genes with this annotation, Figure S8: Molybdopterin biosynthesis-related enzymes in stramenopiles. Heatmap of the presence and absence of the enzymes relating to molybdopterin biosynthesis in the stramenopiles. The yellow gradient represents the ratio of predicted positive selection in genes with this annotation, Figure S9: Glycolysis I, II and III-related enzymes in stramenopiles. Heatmap of the presence and absence of the enzymes relating to the glycolysis pathway in the stramenopiles. The yellow gradient represents the normalized ratio of predicted positive selection in genes with this annotation, Table S1: Summary of the basidiomycete dataset, Table S2: Summary of genomes used for the lifestyle model construction, Table S3: Significant GO terms with a depth higher than 7 found enriched in the

positively selected proteins in plant fungal pathogens, Table S4: Significantly enriched terms relating to biological processes in the positively selected obligate biotroph proteins, Table S5: Significantly enriched terms relating to biological processes in the positively selected hemibiotroph proteins, Table S6: Enriched terms relating to biological processes in the positively selected plant necrotrophs, Table S7: Enriched terms relating to biological processes in the positively selected plant necrotrophs (continued), Table S8: Enriched terms relating to biological processes in the positively selected animal necrotrophs, Table S9: Enriched terms relating to biological processes in the positively selected animal necrotrophs (continued), Table S10: Significant enriched terms relating to biological processes in the stramenopile dataset's paralogs.

Abbreviations

The following abbreviations are used in this manuscript:

CAZyme	Carbohydrate-Active enZyme
GO	Gene Ontology
THF	tetrahydrofolate
UPGMA	Unweighted Pair Group Method with Arithmetic Mean

Appendix A. Stramenopile Dataset

Table A1. Stramenopile genomes dataset used for positive selection analyses.

Phylogenetic Family	Species Name	Accession	Lifestyle	Complete BUSCOs	Complete and Single-Copy BUSCOs	Complete and Duplicated BUSCOs	Reference
Non-oomycete	Ectocarpus siliculosus	GCA_000310025.1	Autotroph	97	97	0	[98]
	Fistulifera solaris	GCA_002217885.1	Autotroph	97	14	83	[62]
	Fragilariopsis cylindrus	GCA_001750085.1	Autotroph	95	95	0	[99]
	Hondaea fermentalgiana	GCA_002897355.1	Autotroph	95	90	5	[100]
	Microchloropsis salina	GCA_004565275.1	Autotroph	92	90	2	[101]
	Phaeodactylum tricornutum	GCA_000150955.2	Autotroph	97	95	2	[102]
	Thalassiosira oceanica	GCA_000296195.2	Autotroph	90	90	0	[103]
	Thalassiosira pseudonana	GCA_000149405.2	Autotroph	97	95	2	[102]
Saprolegniaceae	Achlya hypogyna	GCA_002081595.1	Animal necrotroph [20]	99	98	1	[20]
	Aphanomyces astaci	GCA_000520075.1	Animal necrotroph [104]	100	82	18	
	Aphanomyces euteiches	GCA_009835175.1	Plant necrotroph [19]	99	99	0	
	Aphanomyces invadans	GCA_000520115.1	Animal necrotroph	100	83	17	
	Aphanomyces stellatus	GCA_009835185.1	Plant necrotroph [19]	97	96	1	
	Saprolegnia diclina	GCA_000281045.1	Animal necrotroph [105]	99	98	1	
	Saprolegnia parasitica	GCA_000151545.2	Animal necrotroph [105]	99	99	0	[106]
	Thraustotheca clavata	GCA_002081575.1	Free-living saprotroph [20]	99	98	1	[20]
Albuginaceae	Albugo candida	GCA_001078535.1	Obligate biotroph [107]	98	86	12	
	Albugo laibachii	PRJEA53219	Obligate biotroph [107]	95	82	13	[108]
Peronosporaceae	Bremia lactucae	GCA_004359215.1	Obligate biotroph [109]	96	90	6	[110]
	Globisporangium irregulare	GCA_000387425.2	Plant necrotroph [111]	98	96	2	[112]
	Globisporangium splendens	GCA_006386115.1	Plant necrotroph [113]	91	74	17	[114]
	Globisporangium ultimum	GCA_000143045.1	Plant necrotroph [115]	94	93	1	[112]
	Hyaloperonospora arabidopsidis	GCA_000173235.2	Obligate biotroph [116]	89	82	7	[116]
	Nothophytophthora sp.	GCA_001712635.2		90	28	62	[61]
	Peronospora effusa	GCA_003843895.1	Obligate biotroph [117]	94	93	1	
	Phytophthora cactorum	GCA_003287315.1	Hemibiotroph [118]	100	98	2	[119]
	Phytophthora capsici	GCA_000325885.1	Hemibiotroph [120]	98	97	1	[121]
	Phytophthora cinnamomi	GCA_001314365.1	Hemibiotroph [122]	96	94	2	[123]
	Phytophthora fragariae	GCA_009729455.1	Hemibiotroph	94	93	1	[124]
	Phytophthora infestans	GCA_000142945.1	Hemibiotroph [125]	100	99	1	
	Phytophthora kernoviae	GCA_001712645.2	Hemibiotroph [126]	96	96	0	[61]
	Phytophthora megakarya	GCA_002215365.1	Hemibiotroph	91	90	1	[127]
	Phytophthora nicotianae	GCA_001483015.1	Hemibiotroph [128]	99	86	13	[129]
	Phytophthora parasitica	GCA_000247585.2	Hemibiotroph [130]	98	87	11	
	Phytophthora rubi	GCA_009733145.1	Hemibiotroph	100	98	2	[124]
	Phytophthora sojae	GCA_000149755.2	Hemibiotroph [131]	99	98	1	[132]
	Phytopythium vexans	GCA_000387545.2	Plant necrotroph [17]	94	92	2	[17]
	Pythium brassicum	GCA_008271595.1	Plant necrotroph [133]	100	99	1	
	Plasmopara halstedii	GCA_900000015.1	Obligate biotroph [134]	100	100	0	
Pythiaceae	Pythium aphanidermatum	GCA_000387445.2	Plant necrotroph [135]	94	93	1	[17]
	Pythium insidiosum	GCA_001029375.1	Animal necrotroph [136]	99	87	12	[137]
	Pythium oligandrum	GCA_005966545.1	Fungal necrotroph [138]	100	100	0	[139]

References

1. Zhang, W.; Zhang, X.; Li, K.; Wang, C.; Cai, L.; Zhuang, W.; Xiang, M.; Liu, X. Introgression and gene family contraction drive the evolution of lifestyle and host shifts of hypocrealean fungi. *Mycology* **2018**, *9*, 176–188. [CrossRef]
2. Props, R.; Monsieurs, P.; Vandamme, P.; Leys, N.; Denef, V.J.; Boon, N. Gene Expansion and Positive Selection as Bacterial Adaptations to Oligotrophic Conditions. *mSphere* **2019**, *4*. [CrossRef]
3. Scannell, D.R.; Byrne, K.P.; Gordon, J.L.; Wong, S.; Wolfe, K.H. Multiple rounds of speciation associated with reciprocal gene loss in polyploid yeasts. *Nature* **2006**, *440*, 341–345. [CrossRef] [PubMed]
4. Treangen, T.J.; Rocha, E.P.C. Horizontal Transfer, Not Duplication, Drives the Expansion of Protein Families in Prokaryotes. *PLoS Genet.* **2011**, *7*, e1001284. [CrossRef] [PubMed]
5. Sheridan, P.O.; Raguideau, S.; Quince, C.; Holden, J.; Zhang, L.; Gaze, W.H.; Holden, J.; Mead, A.; Raguideau, S.; Quince, C.; et al. Gene duplication drives genome expansion in a major lineage of Thaumarchaeota. *Nat. Commun.* **2020**, *11*, 5494. [CrossRef]
6. Behe, M. Experimental evolution, loss-of-function mutations, and "the first rule of adaptive evolution". *Q. Rev. Biol.* **2010**, *85*, 419–445. [CrossRef]
7. Yang, Z. Likelihood ratio tests for detecting positive selection and application to primate lysozyme evolution. *Mol. Biol. Evol.* **1998**, *15*, 568–573. [CrossRef]
8. Hughes, A.L.; Packer, B.; Welch, R.; Bergen, A.W.; Chanock, S.J.; Yeager, M. Widespread purifying selection at polymorphic sites in human protein-coding loci. *Proc. Natl. Acad. Sci. USA* **2003**, *100*, 15754–15757. [CrossRef] [PubMed]
9. Kosiol, C.; Vinař, T.; da Fonseca, R.R.; Hubisz, M.J.; Bustamante, C.D.; Nielsen, R.; Siepel, A. Patterns of Positive Selection in Six Mammalian Genomes. *PLoS Genet.* **2008**, *4*, e1000144. [CrossRef]
10. Cavalier-Smith, T.; Chao, E.E.Y. Phylogeny and Megasystematics of Phagotrophic Heterokonts (Kingdom Chromista). *J. Mol. Evol.* **2006**, *62*, 388–420. [CrossRef]
11. Beakes, G.W.; Thines, M. *Handbook of the Protists*; Springer: Cham, Switzerland, 2017; pp. 435–505._26. [CrossRef]
12. Matari, N.H.; Blair, J.E. A multilocus timescale for oomycete evolution estimated under three distinct molecular clock models. *BMC Evol. Biol.* **2014**, *14*, 101. [CrossRef]
13. Bebber, D.P.; Gurr, S.J. Crop-destroying fungal and oomycete pathogens challenge food security. *Fungal Genet. Biol.* **2015**, *74*, 62–64. [CrossRef]
14. Derevnina, L.; Petre, B.; Kellner, R.; Dagdas, Y.F.; Sarowar, M.N.; Giannakopoulou, A.; De la Concepcion, J.C.; Chaparro-Garcia, A.; Pennington, H.G.; Van West, P.; et al. Emerging oomycete threats to plants and animals. *Philos. Trans. R. Soc. B Biol. Sci.* **2016**, *371*, 20150459. [CrossRef]
15. Kemen, E.; Jones, J.D. Obligate biotroph parasitism: Can we link genomes to lifestyles? *Trends Plant Sci.* **2012**, *17*, 448–457. [CrossRef]
16. Lee, S.J.; Rose, J.K.C. Mediation of the transition from biotrophy to necrotrophy in hemibiotrophic plant pathogens by secreted effector proteins. *Plant Signal. Behav.* **2010**, *5*, 769–772. [CrossRef]
17. Adhikari, B.N.; Hamilton, J.P.; Zerillo, M.M.; Tisserat, N.; Lévesque, C.A.; Buell, C.R. Comparative Genomics Reveals Insight into Virulence Strategies of Plant Pathogenic Oomycetes. *PLoS ONE* **2013**, *8*, e75072. [CrossRef]
18. Steciow, M.M.; Lara, E.; Paul, C.; Pillonel, A.; Belbahri, L. Multiple barcode assessment within the Saprolegnia-Achlya clade (Saprolegniales, Oomycota, Straminipila) brings order in a neglected group of pathogens. *IMA Fungus* **2014**, *5*, 439–448. [CrossRef]
19. Gaulin, E.; Jacquet, C.; Bottin, A.; Dumas, B. Root rot disease of legumes caused by Aphanomyces euteiches. *Mol. Plant Pathol.* **2007**, *8*, 539–548. [CrossRef] [PubMed]
20. Misner, I.; Blouin, N.; Leonard, G.; Richards, T.A.; Lane, C.E. The Secreted Proteins of Achlya hypogyna and Thraustotheca clavata Identify the Ancestral Oomycete Secretome and Reveal Gene Acquisitions by Horizontal Gene Transfer. *Genome Biol. Evol.* **2015**, *7*, 120–135. [CrossRef] [PubMed]
21. McGowan, J.; O'Hanlon, R.; Owens, R.A.; Fitzpatrick, D.A. Comparative Genomic and Proteomic Analyses of Three Widespread Phytophthora Species: Phytophthora chlamydospora, Phytophthora gonapodyides and Phytophthora pseudosyringae. *Microorganisms* **2020**, *8*, 653. [CrossRef] [PubMed]
22. Weiblen, C.; Robe, L.J.; de Azevedo, M.I.; Ianiski, L.B.; Stibbe, P.C.; Ribeiro, T.C.; Zanette, R.A.; Pereira, D.I.B.; Santurio, J.M.; Botton, S.D.A. New insights on evolutionary aspects of *Pythium insidiosum* and other peronosporaleans. *Mycoses* **2020**. [CrossRef]
23. Thines, M. An evolutionary framework for host shifts—Jumping ships for survival. *New Phytol.* **2019**, *224*. [CrossRef]
24. Haas, B.J.; Kamoun, S.; Zody, M.C.; Jiang, R.H.Y.; Handsaker, R.E.; Cano, L.M.; Grabherr, M.; Kodira, C.D.; Raffaele, S.; Torto-Alalibo, T.; et al. Genome sequence and analysis of the Irish potato famine pathogen *Phytophthora infestans*. *Nature* **2009**, *461*, 393–398. [CrossRef]
25. Richards, T.A.; Soanes, D.M.; Jones, M.D.M.; Vasieva, O.; Leonard, G.; Paszkiewicz, K.; Foster, P.G.; Hall, N.; Talbot, N.J. Horizontal gene transfer facilitated the evolution of plant parasitic mechanisms in the oomycetes. *Proc. Natl. Acad. Sci. USA* **2011**, *108*, 15258–15263. [CrossRef]
26. Savory, F.; Leonard, G.; Richards, T.A. The Role of Horizontal Gene Transfer in the Evolution of the Oomycetes. *PLoS Pathog.* **2015**, *11*, e1004805. [CrossRef]

27. Savory, E.A.; Fuller, S.L.; Weisberg, A.J.; Thomas, W.J.; Gordon, M.I.; Stevens, D.M.; Creason, A.L.; Belcher, M.S.; Serdani, M.; Wiseman, M.S.; et al. Evolutionary transitions between beneficial and phytopathogenic Rhodococcus challenge disease management. *eLife* **2017**, *6*, e30925. [CrossRef] [PubMed]

28. Money, N.P.; Davis, C.M.; Ravishankar, J. Biomechanical evidence for convergent evolution of the invasive growth process among fungi and oomycete water molds. *Fungal Genet. Biol.* **2004**, *41*, 872–876. [CrossRef] [PubMed]

29. Latijnhouwers, M.; de Wit, P.J.; Govers, F. Oomycetes and fungi: Similar weaponry to attack plants. *Trends Microbiol.* **2003**, *11*, 462–469. [CrossRef]

30. Richards, T.A.; Dacks, J.B.; Jenkinson, J.M.; Thornton, C.R.; Talbot, N.J. Evolution of Filamentous Plant Pathogens: Gene Exchange across Eukaryotic Kingdoms. *Curr. Biol.* **2006**, *16*, 1857–1864. [CrossRef] [PubMed]

31. Seppey, M.; Manni, M.; Zdobnov, E.M. Gene Prediction, Methods and Protocols. *Methods Mol. Biol.* **2019**, *1962*, 227–245. [CrossRef]

32. Jones, P.; Binns, D.; Chang, H.Y.; Fraser, M.; Li, W.; McAnulla, C.; McWilliam, H.; Maslen, J.; Mitchell, A.; Nuka, G.; et al. InterProScan 5: Genome-scale protein function classification. *Bioinformatics* **2014**, *30*, 1236–1240. [CrossRef] [PubMed]

33. Altschul, S.F.; Gish, W.; Miller, W.; Myers, E.W.; Lipman, D.J. Basic local alignment search tool. *J. Mol. Biol.* **1990**, *215*, 403–410. [CrossRef]

34. Petersen, T.N.; Brunak, S.; Von Heijne, G.; Nielsen, H. SignalP 4.0: Discriminating signal peptides from transmembrane regions. *Nat. Methods* **2011**, *8*, 785–786. [CrossRef] [PubMed]

35. Nur, M.; Wood, K.; Michelmore, R. EffectorO: Motif-independent prediction of effectors in oomycete genomes using machine learning and lineage specificity. *BioRxiv* **2021**. [CrossRef]

36. Richardson, L.J.; Rawlings, N.D.; Salazar, G.A.; Almeida, A.; Haft, D.R.; Ducq, G.; Sutton, G.G.; Finn, R.D. Genome properties in 2019: A new companion database to InterPro for the inference of complete functional attributes. *Nucleic Acids Res.* **2018**, *47*, D564–D572. [CrossRef]

37. Virtanen, P.; Gommers, R.; Oliphant, T.E.; Haberland, M.; Reddy, T.; Cournapeau, D.; Burovski, E.; Peterson, P.; Weckesser, W.; Bright, J.; et al. SciPy 1.0: Fundamental Algorithms for Scientific Computing in Python. *Nat. Methods* **2020**, *17*, 261–272. [CrossRef] [PubMed]

38. Robinson, D.; Foulds, L. Comparison of phylogenetic trees. *Math. Biosci.* **1981**, *53*, 131–147. [CrossRef]

39. Goluch, T.; Bogdanowicz, D.; Giaro, K. Visual TreeCmp: Comprehensive Comparison of Phylogenetic Trees on the Web. *Methods Ecol. Evol.* **2020**, *11*, 494–499. [CrossRef]

40. Minh, B.Q.; Schmidt, H.A.; Chernomor, O.; Schrempf, D.; Woodhams, M.D.; Von Haeseler, A..; Lanfear, R. IQ-TREE 2: New models and efficient methods for phylogenetic inference in the genomic era. *Mol. Biol. Evol.* **2020**, *37*, 1530–1534. [CrossRef]

41. Köster, J.; Rahmann, S. Snakemake—A scalable bioinformatics workflow engine. *Bioinformatics* **2012**, *28*, 2520–2522. [CrossRef]

42. Katoh, K.; Asimenos, G.; Toh, H. Multiple alignment of DNA sequences with MAFFT. *Methods Mol. Biol.* **2009**, *537*, 39–64. [CrossRef] [PubMed]

43. Price, M.N.; Dehal, P.S.; Arkin, A.P. FastTree 2—Approximately Maximum-Likelihood Trees for Large Alignments. *PLoS ONE* **2010**, *5*, e9490. [CrossRef] [PubMed]

44. Suyama, M.; Torrents, D.; Bork, P. PAL2NAL: Robust conversion of protein sequence alignments into the corresponding codon alignments. *Nucleic Acids Res.* **2006**, *34*, W609–W612. [CrossRef] [PubMed]

45. Lechner, M.; Findeiß, S.; Steiner, L.; Marz, M.; Stadler, P.F.; Prohaska, S.J. Proteinortho: Detection of (Co-)orthologs in large-scale analysis. *BMC Bioinform.* **2011**, *12*, 124. [CrossRef] [PubMed]

46. Smith, M.D.; Wertheim, J.O.; Weaver, S.; Murrell, B.; Scheffler, K.; Pond, S.L.K. Less Is More: An Adaptive Branch-Site Random Effects Model for Efficient Detection of Episodic Diversifying Selection. *Mol. Biol. Evol.* **2015**, *32*, 1342–1353. [CrossRef] [PubMed]

47. Murrell, B.; Moola, S.; Mabona, A.; Weighill, T.; Sheward, D.; Pond, S.L.K.; Scheffler, K. FUBAR: A Fast, Unconstrained Bayesian AppRoximation for Inferring Selection. *Mol. Biol. Evol.* **2013**, *30*, 1196–1205. [CrossRef] [PubMed]

48. Ashburner, M.; Ball, C.A.; Blake, J.A.; Botstein, D.; Butler, H.; Cherry, J.M.; Davis, A.P.; Dolinski, K.; Dwight, S.S.; Eppig, J.T.; et al. Gene Ontology: Tool for the unification of biology. *Nat. Genet.* **2000**, *25*, 25–29. [CrossRef]

49. Carbon, S.; Douglass, E.; Dunn, N.; Good, B.; Harris, N.L.; Lewis, S.E.; Mungall, C.J.; Basu, S.; Chisholm, R.L.; Dodson, R.J.; et al. The Gene Ontology Resource: 20 years and still GOing strong. *Nucleic Acids Res.* **2018**, *47*, gky1055. [CrossRef]

50. Klopfenstein, D.V.; Zhang, L.; Pedersen, B.S.; Ramírez, F.; Vesztrocy, A.W.; Naldi, A.; Mungall, C.J.; Yunes, J.M.; Botvinnik, O.; Weigel, M.; et al. GOATOOLS: A Python library for Gene Ontology analyses. *Sci. Rep.* **2018**, *8*, 10872. [CrossRef]

51. Hunter, S.; Apweiler, R.; Attwood, T.K.; Bairoch, A.; Bateman, A.; Binns, D.; Bork, P.; Das, U.; Daugherty, L.; Duquenne, L.; et al. InterPro: The integrative protein signature database. *Nucleic Acids Res.* **2009**, *37*, D211–D215. [CrossRef]

52. Abadi, M.; Agarwal, A.; Barham, P.; Brevdo, E.; Chen, Z.; Citro, C.; Corrado, G.S.; Davis, A.; Dean, J.; Devin, M.; et al. TensorFlow: Large-Scale Machine Learning on Heterogeneous Systems. 2015. Available online: tensorflow.org (accessed on 24 June 2021).

53. Zhang, H.; Yohe, T.; Huang, L.; Entwistle, S.; Wu, P.; Yang, Z.; Busk, P.K.; Xu, Y.; Yin, Y. dbCAN2: A meta server for automated carbohydrate-active enzyme annotation. *Nucleic Acids Res.* **2018**, *46*, gky418. [CrossRef]

54. O'Malley, T.; Bursztein, E.; Long, J.; Chollet, F.; Jin, H.; Invernizzi, L.; et al. Keras Tuner. 2019. Available online: https://github.com/keras-team/keras-tuner (accessed on 24 June 2021).

55. Li, L.; Jamieson, K.; DeSalvo, G.; Rostamizadeh, A.; Talwalkar, A. Hyperband: A Novel Bandit-Based Approach to Hyperparameter Optimization. *J. Mach. Learn. Res.* **2018**, *18*, 6765–6816.

56. Basenko, E.; Pulman, J.; Shanmugasundram, A.; Harb, O.; Crouch, K.; Starns, D.; Warrenfeltz, S.; Aurrecoechea, C.; Stoeckert, C.; Kissinger, J.; et al. FungiDB: An Integrated Bioinformatic Resource for Fungi and Oomycetes. *J. Fungi* **2018**, *4*, 39. [CrossRef] [PubMed]

57. O'Leary, N.A.; Wright, M.W.; Brister, J.R.; Ciufo, S.; Haddad, D.; McVeigh, R.; Rajput, B.; Robbertse, B.; Smith-White, B.; Ako-Adjei, D.; et al. Reference sequence (RefSeq) database at NCBI: Current status, taxonomic expansion, and functional annotation. *Nucleic Acids Res.* **2016**, *44*, D733–D745. [CrossRef] [PubMed]

58. De Cock, A.; Lodhi, A.; Rintoul, T.; Bala, K.; Robideau, G.; Abad, Z.G.; Coffey, M.; Shahzad, S.; Lévesque, C. Phytopythium: Molecular phylogeny and systematics. *Persoonia Mol. Phylogeny Evol. Fungi* **2015**, *34*, 25–39. [CrossRef] [PubMed]

59. McGowan, J.; Fitzpatrick, D.A. Recent advances in oomycete genomics. *Adv. Genet.* **2020**, *105*, 175–228. [CrossRef]

60. Martens, C.; Van de Peer, Y. The hidden duplication past of the plant pathogen Phytophthora and its consequences for infection. *BMC Genom.* **2010**, *11*, 353. [CrossRef]

61. Studholme, D.J.; Panda, P.; Stowasser, E.S.V.; González, M.; Hill, R.; Sambles, C.; Grant, M.; Williams, N.M.; McDougal, R.L. Genome sequencing of oomycete isolates from Chile supports the New Zealand origin of *Phytophthora kernoviae* and makes available the first *Nothophytophthora* sp. genome: Comparative genomics of Chilean oomycete isolates. *Mol. Plant Pathol.* **2018**, *20*, 423–431. [CrossRef]

62. Tanaka, T.; Maeda, Y.; Veluchamy, A.; Tanaka, M.; Abida, H.; Maréchal, E.; Bowler, C.; Muto, M.; Sunaga, Y.; Tanaka, M.; et al. Oil accumulation by the oleaginous diatom *Fistulifera solaris* as revealed by the genome and transcriptome. *Plant Cell* **2015**, *27*, 162–176. [CrossRef]

63. Gaulin, E.; Pel, M.J.C.; Camborde, L.; San-Clemente, H.; Courbier, S.; Dupouy, M.A.; Lengellé, J.; Veyssiere, M.; Ru, A.L.; Grandjean, F.; et al. Genomics analysis of *Aphanomyces* spp. identifies a new class of oomycete effector associated with host adaptation. *BMC Biol.* **2018**, *16*, 43. [CrossRef] [PubMed]

64. Stephenson, S.A.; Green, J.R.; Manners, J.M.; Maclean, D.J. Cloning and characterisation of glutamine synthetase from *Colletotrichum gloeosporioides* and demonstration of elevated expression during pathogenesis on *Stylosanthes guianensis*. *Curr. Genet.* **1997**, *31*, 447–454. [CrossRef]

65. Hallen, H.E.; Huebner, M.; Shiu, S.H.; Güldener, U.; Trail, F. Gene expression shifts during perithecium development in *Gibberella zeae* (anamorph *Fusarium graminearum*), with particular emphasis on ion transport proteins. *Fungal Genet. Biol.* **2007**, *44*, 1146–1156. [CrossRef]

66. Walley, J.W.; Kliebenstein, D.J.; Bostock, R.M.; Dehesh, K. Fatty acids and early detection of pathogens. *Curr. Opin. Plant Biol.* **2013**, *16*, 520–526. [CrossRef]

67. McCutcheon, J.P.; Moran, N.A. Functional Convergence in Reduced Genomes of Bacterial Symbionts Spanning 200 My of Evolution. *Genome Biol. Evol.* **2010**, *2*, 708–718. [CrossRef]

68. Shang, Y.; Xiao, G.; Zheng, P.; Cen, K.; Zhan, S.; Wang, C. Divergent and Convergent Evolution of Fungal Pathogenicity. *Genome Biol. Evol.* **2016**, *8*, 1374–1387. [CrossRef]

69. Rodenburg, S.Y.; De Ridder, D.; Govers, F.; Seidl, M.F. Oomycete metabolism is highly dynamic and reflects lifestyle adaptations. *BioRxiv* **2020**. [CrossRef]

70. Lewis, D.H. Concepts in Fungal Nutrition and the Origin of Biotrophy. *Biol. Rev.* **1973**, *48*, 261–277. [CrossRef]

71. Svoboda, J.; Mrugała, A.; Kozubíková-Balcarová, E.; Petrusek, A. Hosts and transmission of the crayfish plague pathogen *Aphanomyces astaci*: A review. *J. Fish Dis.* **2016**, *40*, 127–140. [CrossRef]

72. Mélida, H.; Sandoval-Sierra, J.V.; Diéguez-Uribeondo, J.; Bulone, V. Analyses of Extracellular Carbohydrates in Oomycetes Unveil the Existence of Three Different Cell Wall Types. *Eukaryot. Cell* **2013**, *12*, 194–203. [CrossRef]

73. Wang, E.; Schornack, S.; Marsh, J.; Gobbato, E.; Schwessinger, B.; Eastmond, P.; Schultze, M.; Kamoun, S.; Oldroyd, G. A Common Signaling Process that Promotes Mycorrhizal and Oomycete Colonization of Plants. *Curr. Biol.* **2012**, *22*, 2242–2246. [CrossRef]

74. Zheng, L.; Mackrill, J.J. Calcium Signaling in Oomycetes: An Evolutionary Perspective. *Front. Physiol.* **2016**, *7*, 123. [CrossRef]

75. Judelson, H.S. Dynamics and Innovations within Oomycete Genomes: Insights into Biology, Pathology, and Evolution. *Eukaryot. Cell* **2012**, *11*, 1304–1312. [CrossRef]

76. Klarzynski, O.; Plesse, B.; Joubert, J.M.; Yvin, J.C.; Kopp, M.; Kloareg, B.; Fritig, B. Linear *β*-1,3 Glucans Are Elicitors of Defense Responses in Tobacco. *Plant Physiol.* **2000**, *124*, 1027–1038. [CrossRef]

77. Précigout, P.A.; Claessen, D.; Makowski, D.; Robert, C. Does the Latent Period of Leaf Fungal Pathogens Reflect Their Trophic Type? A Meta-Analysis of Biotrophs, Hemibiotrophs, and Necrotrophs. *Phytopathology* **2020**, *110*, 345–361. [CrossRef]

78. Xiang, Q.; Judelson, H.S. Myb transcription factors in the oomycete *Phytophthora* with novel diversified DNA-binding domains and developmental stage-specific expression. *Gene* **2010**, *453*, 1–8. [CrossRef]

79. Xiang, Q.; Judelson, H.S. Myb Transcription Factors and Light Regulate Sporulation in the Oomycete *Phytophthora infestans*. *PLoS ONE* **2014**, *9*, e92086. [CrossRef]

80. Rocafort, M.; Fudal, I.; Mesarich, C.H. Apoplastic effector proteins of plant-associated fungi and oomycetes. *Curr. Opin. Plant Biol.* **2020**, *56*, 9–19. [CrossRef]

81. Wang, Y.; Tyler, B.M.; Wang, Y. Defense and Counterdefense during Plant-Pathogenic Oomycete Infection. *Annu. Rev. Microbiol.* **2019**, *73*, 667–696. [CrossRef]

82. Raffaele, S.; Win, J.; Cano, L.M.; Kamoun, S. Analyses of genome architecture and gene expression reveal novel candidate virulence factors in the secretome of *Phytophthora infestans*. *BMC Genom.* **2010**, *11*, 637. [CrossRef] [PubMed]

83. Idänheimo, N.; Gauthier, A.; Salojärvi, J.; Siligato, R.; Brosché, M.; Kollist, H.; Mähönen, A.P.; Kangasjärvi, J.; Wrzaczek, M. The *Arabidopsis thaliana* cysteine-rich receptor-like kinases CRK6 and CRK7 protect against apoplastic oxidative stress. *Biochem. Biophys. Res. Commun.* **2014**, *445*, 457–462. [CrossRef]

84. Grenville-Briggs, L.J.; Avrova, A.O.; Bruce, C.R.; Williams, A.; Whisson, S.C.; Birch, P.R.; van West, P. Elevated amino acid biosynthesis in *Phytophthora infestans* during appressorium formation and potato infection. *Fungal Genet. Biol.* **2005**, *42*, 244–256. [CrossRef] [PubMed]

85. Dahlin, P.; Srivastava, V.; Ekengren, S.; McKee, L.S.; Bulone, V. Comparative analysis of sterol acquisition in the oomycetes *Saprolegnia parasitica* and *Phytophthora infestans*. *PLoS ONE* **2017**, *12*, e0170873. [CrossRef]

86. Daumann, M.; Fischer, M.; Niopek-Witz, S.; Girke, C.; Möhlmann, T. Apoplastic Nucleoside Accumulation in Arabidopsis Leads to Reduced Photosynthetic Performance and Increased Susceptibility against *Botrytis cinerea*. *Front. Plant Sci.* **2015**, *6*, 1158. [CrossRef]

87. Fones, H.; Preston, G.M. Reactive oxygen and oxidative stress tolerance in plant pathogenic *Pseudomonas*. *FEMS Microbiol. Lett.* **2012**, *327*, 1–8. [CrossRef] [PubMed]

88. Gottlieb, D. Differences in the Sterol Synthesizing Pathways of Sterol-Producing and Non-Sterol-Producing Fungi. *Phytopathology* **1978**, *68*, 1168. [CrossRef]

89. Gaulin, E.; Bottin, A.; Dumas, B. Sterol biosynthesis in oomycete pathogens. *Plant Signal. Behav.* **2010**, *5*, 258–260. [CrossRef] [PubMed]

90. Ah-Fong, A.M.V.; Kagda, M.S.; Abrahamian, M.; Judelson, H.S. Niche-specific metabolic adaptation in biotrophic and necrotrophic oomycetes is manifested in differential use of nutrients, variation in gene content, and enzyme evolution. *PLoS Pathog.* **2019**, *15*, e1007729. [CrossRef]

91. Huennekens, F. Folic Acid Coenzymes in the Biosynthesis of Purines and Pyrimidines. *Vitam. Horm.* **1969**, *26*, 375–394. [CrossRef]

92. Schwarz, G.; Mendel, R.R. Molybdenum Cofactor Biosynthesis and Molybdenum Enzymes. *Plant Biol.* **2006**, *57*, 623–647. [CrossRef] [PubMed]

93. Judelson, H.S. Metabolic Diversity and Novelties in the Oomycetes. *Annu. Rev. Microbiol.* **2016**, *71*, 21–39. [CrossRef]

94. Zhang, J.; Rosenberg, H.F.; Nei, M. Positive Darwinian selection after gene duplication in primate ribonuclease genes. *Proc. Natl. Acad. Sci. USA* **1998**, *95*, 3708–3713. [CrossRef]

95. King, B.C.; Waxman, K.D.; Nenni, N.V.; Walker, L.P.; Bergstrom, G.C.; Gibson, D.M. Arsenal of plant cell wall degrading enzymes reflects host preference among plant pathogenic fungi. *Biotechnol. Biofuels* **2011**, *4*, 4. [CrossRef]

96. Hane, J.K.; Paxman, J.; Jones, D.A.B.; Oliver, R.P.; de Wit, P. "CATAStrophy", a Genome-Informed Trophic Classification of Filamentous Plant Pathogens—How Many Different Types of Filamentous Plant Pathogens Are There? *Front. Microbiol.* **2020**, *10*, 3088. [CrossRef]

97. Torruella, G.; de Mendoza, A.; Grau-Bové, X.; Antó, M.; Chaplin, M.; del Campo, J.; Eme, L.; Pérez-Cordón, G.; Whipps, C.; Nichols, K.; et al. Phylogenomics Reveals Convergent Evolution of Lifestyles in Close Relatives of Animals and Fungi. *Curr. Biol.* **2015**, *25*, 2404–2410. [CrossRef] [PubMed]

98. Cock, J.M.; Sterck, L.; Rouzé, P.; Scornet, D.; Allen, A.E.; Amoutzias, G.; Anthouard, V.; Artiguenave, F.; Aury, J.M.; Badger, J.H.; et al. The Ectocarpus genome and the independent evolution of multicellularity in brown algae. *Nature* **2010**, *465*, 617–621. [CrossRef]

99. Mock, T. Extensive genetic diversity and differential bi-allelic expression in a Southern Ocean diatom. *Eur. J. Phycol.* **2015**, *50*, 75.

100. Seddiki, K.; Godart, F.; Cigliano, R.A.; Sanseverino, W.; Barakat, M.; Ortet, P.; Rébeillé, F.; Maréchal, E.; Cagnac, O.; Amato, A. Sequencing, De Novo Assembly, and Annotation of the Complete Genome of a New Thraustochytrid Species, Strain CCAP_4062/3. *Genome Announc.* **2018**, *6*, e01335-17. [CrossRef]

101. Ohan, J.A.; Hovde, B.T.; Zhang, X.L.; Davenport, K.W.; Chertkov, O.; Han, C.; Twary, S.N.; Starkenburg, S.R. Nuclear Genome Assembly of the Microalga Nannochloropsis salina CCMP1776. *Microbiol. Resour. Announc.* **2019**, *8*. [CrossRef]

102. Bowler, C.; Allen, A.E.; Badger, J.H.; Grimwood, J.; Jabbari, K.; Kuo, A.; Maheswari, U.; Martens, C.; Maumus, F.; Otillar, R.P.; et al. The Phaeodactylum genome reveals the evolutionary history of diatom genomes. *Nature* **2008**, *456*, 239–244. [CrossRef]

103. Lommer, M.; Specht, M.; Roy, A.S.; Kraemer, L.; Andreson, R.; Gutowska, M.A.; Wolf, J.; Bergner, S.V.; Schilhabel, M.B.; Klostermeier, U.C.; et al. Genome and low-iron response of an oceanic diatom adapted to chronic iron limitation. *Genome Biol.* **2012**, *13*, R66. [CrossRef]

104. Alderman, D.J.; Polglase, J.L.; Frayling, M. Aphanomyces astaci pathogenicity under laboratory and field conditions. *J. Fish Dis.* **1987**, *10*, 385–393. [CrossRef]

105. Willoughby, L.G. Saprolegnias of salmonid fish in Windermere: A critical analysis. *J. Fish Dis.* **1978**, *1*, 51–67. [CrossRef]

106. Jiang, R.H.Y.; de Bruijn, I.; Haas, B.J.; Belmonte, R.; Löbach, L.; Christie, J.; van den Ackerveken, G.; Bottin, A.; Bulone, V.; Díaz-Moreno, S.M.; et al. Distinctive Expansion of Potential Virulence Genes in the Genome of the Oomycete Fish Pathogen *Saprolegnia parasitica*. *PLoS Genet.* **2013**, *9*, e1003272. [CrossRef]

107. Ruhe, J.; Agler, M.T.; Placzek, A.; Kramer, K.; Finkemeier, I.; Kemen, E.M. Obligate Biotroph Pathogens of the Genus Albugo Are Better Adapted to Active Host Defense Compared to Niche Competitors. *Front. Plant Sci.* **2016**, *7*, 820. [CrossRef]

108. Kemen, E.; Gardiner, A.; Schultz-Larsen, T.; Kemen, A.C.; Balmuth, A.L.; Robert-Seilaniantz, A.; Bailey, K.; Holub, E.; Studholme, D.J.; MacLean, D.; et al. Gene Gain and Loss during Evolution of Obligate Parasitism in the White Rust Pathogen of *Arabidopsis thaliana*. *PLoS Biol.* **2011**, *9*, e1001094. [CrossRef]

109. Francis, D.M.; Hulbert, S.H.; Michelmore, R.W. Genome size and complexity of the obligate fungal pathogen, *Bremia lactucae*. *Exp. Mycol.* **1990**, *14*, 299–309. [CrossRef]

110. Fletcher, K.; Gil, J.; Bertier, L.D.; Kenefick, A.; Wood, K.J.; Zhang, L.; Reyes-Chin-Wo, S.; Cavanaugh, K.; Tsuchida, C.; Wong, J.; et al. Genomic signatures of somatic hybrid vigor due to heterokaryosis in the oomycete pathogen, *Bremia lactucae*. *BioRxiv* **2019**, 516526. [CrossRef]

111. Hancock, J.G. Seedling and Rootlet Diseases of Forage Alfalfa Caused by *Pythium irregulare*. *Plant Dis.* **1991**, *75*, 691. [CrossRef]

112. Lévesque, C.A.; Brouwer, H.; Cano, L.; Hamilton, J.P.; Holt, C.; Huitema, E.; Raffaele, S.; Robideau, G.P.; Thines, M.; Win, J.; et al. Genome sequence of the necrotrophic plant pathogen *Pythium ultimum* reveals original pathogenicity mechanisms and effector repertoire. *Genome Biol.* **2010**, *11*, R73. [CrossRef] [PubMed]

113. Linde, C. Root and Root Collar Disease of *Eucalyptus grandis* Caused by *Pythium splendens*. *Plant Dis.* **1994**, *78*, 10061. [CrossRef]

114. Reghu, R.J.; Chellappan, B.V.; Beena, S.H.; Sasi, A.; Vasudevan, S.E.; Nair, A.S. Draft Genome Sequence of the Oomycete *Globisporangium splendens* Strain rgcb-1. *Microbiol. Resour. Announc.* **2020**, *9*. [CrossRef]

115. Howell, C.R. Suppression of *Pythium ultimum*-Induced Damping-Off of Cotton Seedlings by *Pseudomonas fluorescens* and its Antibiotic, Pyoluteorin. *Phytopathology* **1980**, *70*, 712. [CrossRef]

116. Baxter, L.; Tripathy, S.; Ishaque, N.; Boot, N.; Cabral, A.; Kemen, E.; Thines, M.; Ah-Fong, A.; Anderson, R.; Badejoko, W.; et al. Signatures of Adaptation to Obligate Biotrophy in the *Hyaloperonospora arabidopsidis* Genome. *Science* **2010**, *330*, 1549–1551. [CrossRef]

117. Lyon, R.; Correll, J.; Feng, C.; Bluhm, B.; Shrestha, S.; Shi, A.; Lamour, K. Population Structure of *Peronospora effusa* in the Southwestern United States. *PLoS ONE* **2016**, *11*, e0148385. [CrossRef]

118. Chen, X.R.; Zhang, B.Y.; Xing, Y.P.; Li, Q.Y.; Li, Y.P.; Tong, Y.H.; Xu, J.Y. Transcriptomic analysis of the phytopathogenic oomycete *Phytophthora cactorum* provides insights into infection-related effectors. *BMC Genom.* **2014**, *15*, 980. [CrossRef] [PubMed]

119. Armitage, A.D.; Lysøe, E.; Nellist, C.F.; Lewis, L.A.; Cano, L.M.; Harrison, R.J.; Brurberg, M.B. Bioinformatic characterisation of the effector repertoire of the strawberry pathogen *Phytophthora cactorum*. *PLoS ONE* **2018**, *13*, e0202305. [CrossRef]

120. Chen, X.R.; Huang, S.X.; Zhang, Y.; Sheng, G.L.; Li, Y.P.; Zhu, F. Identification and functional analysis of the NLP-encoding genes from the phytopathogenic oomycete *Phytophthora capsici*. *Mol. Genet. Genom.* **2018**, *293*, 931–943. [CrossRef] [PubMed]

121. Lamour, K.H.; Mudge, J.; Gobena, D.; Hurtado-Gonzales, O.P.; Schmutz, J.; Kuo, A.; Miller, N.A.; Rice, B.J.; Raffaele, S.; Cano, L.M.; et al. Genome Sequencing and Mapping Reveal Loss of Heterozygosity as a Mechanism for Rapid Adaptation in the Vegetable Pathogen *Phytophthora capsici*. *Mol. Plant-Microbe Interact.* **2012**, *25*, 1350–1360. [CrossRef]

122. Santos, C.; Duarte, S.; Tedesco, S.; Fevereiro, P.; Costa, R.L. Expression Profiling of *Castanea* Genes during Resistant and Susceptible Interactions with the Oomycete Pathogen *Phytophthora cinnamomi* Reveal Possible Mechanisms of Immunity. *Front. Plant Sci.* **2017**, *8*, 515. [CrossRef]

123. Studholme, D.; McDougal, R.; Sambles, C.; Hansen, E.; Hardy, G.; Grant, M.; Ganley, R.; Williams, N. Genome sequences of six *Phytophthora* species associated with forests in New Zealand. *Genom. Data* **2016**, *7*, 54–56. [CrossRef]

124. Adams, T.M.; Armitage, A.D.; Sobczyk, M.K.; Bates, H.J.; Tabima, J.F.; Kronmiller, B.A.; Tyler, B.M.; Grünwald, N.J.; Dunwell, J.M.; Nellist, C.F.; et al. Genomic Investigation of the Strawberry Pathogen *Phytophthora fragariae* Indicates Pathogenicity Is Associated with Transcriptional Variation in Three Key Races. *Front. Microbiol.* **2020**, *11*, 490. [CrossRef] [PubMed]

125. Zuluaga, A.P.; Vega-Arreguín, J.C.; Fei, Z.; Ponnala, L.; Lee, S.J.; Matas, A.J.; Patev, S.; Fry, W.E.; Rose, J.K.C. Transcriptome of *P. infestans* in tomato. *Mol. Plant Pathol.* **2016**, *17*, 29–41. [CrossRef]

126. Denman, S.; Kirk, S.A.; Moralejo, E.; Webber, J.F. *Phytophthora ramorum* and *Phytophthora kernoviae* on naturally infected asymptomatic foliage. *EPPO Bull.* **2009**, *39*, 105–111. [CrossRef]

127. Ali, S.S.; Shao, J.; Lary, D.J.; Kronmiller, B.A.; Shen, D.; Strem, M.D.; Amoako-Attah, I.; Akrofi, A.Y.; Begoude, B.D.; Ten Hoopen, G.M.; et al. Phytophthora megakarya and Phytophthora palmivora, Closely Related Causal Agents of Cacao Black Pod Rot, Underwent Increases in Genome Sizes and Gene Numbers by Different Mechanisms. *Genome Biol. Evol.* **2017**, *9*, 536–557. [CrossRef]

128. Jimenez-Lopez, J.C.; Melser, S.; DeBoer, K.; Thatcher, L.F.; Kamphuis, L.G.; Foley, R.C.; Singh, K.B. Narrow-Leafed Lupin (*Lupinus angustifolius*) β1- and β6-Conglutin Proteins Exhibit Antifungal Activity, Protecting Plants against Necrotrophic Pathogen Induced Damage from *Sclerotinia sclerotiorum* and *Phytophthora nicotianae*. *Front. Plant Sci.* **2016**, *7*, 1856. [CrossRef]

129. Liu, H.; Ma, X.; Yu, H.; Fang, D.; Li, Y.; Wang, X.; Wang, W.; Dong, Y.; Xiao, B. Genomes and virulence difference between two physiological races of *Phytophthora nicotianae*. *GigaScience* **2016**, *5*, 3. [CrossRef]

130. Cho, K.; Kim, Y.; Wi, S.J.; Seo, J.B.; Kwon, J.; Chung, J.H.; Park, K.Y.; Nam, M.H. Metabolic Survey of Defense Responses to a Compatible Hemibiotroph, *Phytophthora parasitica* var. *nicotianae*, in Ethylene Signaling-Impaired Tobacco. *J. Agric. Food Chem.* **2013**, *61*, 8477–8489. [CrossRef]

131. Moy, P.; Qutob, D.; Chapman, B.P.; Atkinson, I.; Gijzen, M. Patterns of Gene Expression Upon Infection of Soybean Plants by *Phytophthora sojae*. *Mol. Plant-Microbe Interact.* **2004**, *17*, 1051–1062. [CrossRef] [PubMed]

132. Tyler, B.M.; Tripathy, S.; Zhang, X.; Dehal, P.; Jiang, R.H.Y.; Aerts, A.; Arredondo, F.D.; Baxter, L.; Bensasson, D.; Beynon, J.L.; et al. *Phytophthora* Genome Sequences Uncover Evolutionary Origins and Mechanisms of Pathogenesis. *Science* **2006**, *313*, 1261–1266. [CrossRef]

133. Stanghellini, M.E.; Mohammadi, M.; Förster, H.; Adaskaveg, J.E. *Pythium brassicum* sp. nov.: A Novel Plant Family-Specific Root Pathogen. *Plant Dis.* **2014**, *98*, 1619–1625. [CrossRef] [PubMed]

134. Delmotte, F.; Giresse, X.; Richard-Cervera, S.; M'Baya, J.; Vear, F.; Tourvieille, J.; Walser, P.; de Labrouhe, D.T. Single nucleotide polymorphisms reveal multiple introductions into France of *Plasmopara halstedii*, the plant pathogen causing sunflower downy mildew. *Infect. Genet. Evol.* **2008**, *8*, 534–540. [CrossRef] [PubMed]

135. El-Tarabily, K.; Nassar, A.; Hardy, G.; Sivasithamparam, K. Plant growth promotion and biological control of *Pythium aphanider-matum*, a pathogen of cucumber, by endophytic actinomycetes. *J. Appl. Microbiol.* **2009**, *106*, 13–26. [CrossRef] [PubMed]

136. Gaastra, W.; Lipman, L.J.; Cock, A.W.D.; Exel, T.K.; Pegge, R.B.; Scheurwater, J.; Vilela, R.; Mendoza, L. *Pythium insidiosum*: An overview. *Vet. Microbiol.* **2010**, *146*, 1–16. [CrossRef]

137. Rujirawat, T.; Patumcharoenpol, P.; Lohnoo, T.; Yingyong, W.; Lerksuthirat, T.; Tangphatsornruang, S.; Suriyaphol, P.; Grenville-Briggs, L.J.; Garg, G.; Kittichotirat, W.; et al. Draft Genome Sequence of the Pathogenic Oomycete *Pythium insidiosum* Strain Pi-S, Isolated from a Patient with Pythiosis. *Genome Announc.* **2015**, *3*, e00574-15. [CrossRef]

138. Deacon, J. Studies on *Pythium oligandrum*, an aggressive parasite of other fungi. *Trans. Br. Mycol. Soc.* **1976**, *66*, 383–391. [CrossRef]

139. Faure, C.; Veyssière, M.; Boëlle, B.; San Clemente, H.; Bouchez, O.; Lopez-Roques, C.; Chaubet, A.; Martinez, Y.; Bezouška, K.; Suchánek, M.; et al. Long-Read Genome Sequence of the Sugar Beet Rhizosphere Mycoparasite *Pythium oligandrum*. *G3 Genes Genomes Genet.* **2020**, *10*, 431–436. [CrossRef]